

0.0001). At 28 days after cultivation, the compression modulus of samples with seeded chondrocytes in the 100  $\mu\text{m}$  group, 200  $\mu\text{m}$  group, and 400  $\mu\text{m}$  group was  $2.25 \pm 0.74$  MPa,  $1.82 \pm 0.71$  MPa, and  $1.06 \pm 0.41$  MPa, respectively. The value in the 100  $\mu\text{m}$  group was significantly higher than that in the 400  $\mu\text{m}$  group ( $p < 0.05$ ). However, while the compression modulus of the 400  $\mu\text{m}$  group tended to increase after 4 weeks cultivation, the value of the 100  $\mu\text{m}$  group significantly decreased after cultivation ( $p < 0.0001$ ).

## DISCUSSION

In articular cartilage tissue engineering, we must consider that the articular cartilage is adapted to withstand enormous mechanical stress. Therefore, to maintain the initial shape of the scaffold surface and the number of attached chondrocytes, adequate mechanical strength and high cellular adhesivity are requirements for cartilage tissue engineering scaffold materials. Moreover, for successful cartilage tissue regeneration, the other consideration is to prevent the dedifferentiation of seeded chondrocytes into fibroblast-like cells in order to maintain their chondrocyte phenotype. To achieve these biomechanical and biological requirements, we originally developed the chitosan-based hyaluronic acid hybrid polymer fibers.<sup>7</sup> Our previous study showed their superior adhesivity of chondrocytes and ability of maintaining the chondrocyte phenotype.<sup>7</sup> In the current study, using these fibers as basic materials, we successfully developed 3-D fabricated scaffolds with different pore sizes.

The current study clarified that the pore size of the novel fabricated scaffolds affected the chondrocyte behaviors cultured onto these scaffolds. The cellular adhesivity of the scaffold with 400  $\mu\text{m}$  pore size significantly decreased, compared with that of the scaffolds with 100 and 200  $\mu\text{m}$  pore sizes. Regarding the chondrocyte proliferation, the amount of DNA at 7 and 14 days of culture was significantly higher in the 100  $\mu\text{m}$  group than in the 400  $\mu\text{m}$  group. On the other hand, at 28 days of culture, no significant difference in the value was found among the scaffolds. In this culture period, these results indicate that the current scaffold with 400  $\mu\text{m}$  pore size enhances the chondrocyte proliferation, as compared to that with 100  $\mu\text{m}$  pore size. On the other hand, GAG content significantly increased during the culture period for the 400  $\mu\text{m}$  group compared with the other groups. In addition, the ratio of type II/I collagen mRNA level was significantly higher in the 400  $\mu\text{m}$  group than in other groups. On the basis of these results, we reasonably conclude that our 3-D scaffold with 400  $\mu\text{m}$  pore size significantly enhances ECM synthesis by chondrocytes.

As mentioned above, the scaffold pore size is highly interconnected with cell proliferation and ECM production in chondrocyte culture. Several studies have shown this point using various scaffold materials.<sup>11-13</sup> Nehrer et al.<sup>11</sup> reported on the effects of pore size, which was from 20 to 86  $\mu\text{m}$ , on the chondrocyte behaviors by using collagen sponges. They concluded that small pore diameter affected morphology initially in the type I collagen matrices and showed a higher increase of DNA content, but with time the cell lost the chondrocytic morphology. Bhardwaj et al.<sup>12</sup> showed that porous titanium alloy discs with small pore sizes (13  $\mu\text{m}$ ) significantly increased the amounts of proteoglycan and DNA contents, compared with that with large pore sizes (68  $\mu\text{m}$ ). However, the amount of collagen accumulated per cell was less in the tissue formed on the small pore size discs as compared with the tissue formation on the discs with larger pore sizes. Using the poly(ethylene glycol)-terephthalate/poly(butylene terephthalate) scaffolds with different pore sizes (182 and 525  $\mu\text{m}$ ), Malda et al.<sup>13</sup> demonstrated the weight ratio of GAG/DNA was significantly higher in large pore scaffolds after subcutaneous implantation. These results suggest that the effects of pore sizes of scaffolds on chondrocyte behaviors depend on the basic material constituting the scaffold. It must be noted that these results are strongly dependent on the design of the scaffold and chondrogenic ability of the material. A significance of the current study was to determine the biological effects of pore size on chondrocyte behaviors cultured in a novel 3-D fabricated scaffold created from the chitosan-based hyaluronic acid hybrid polymer fibers.

Scaffolds designed for articular cartilage tissue engineering ideally provide mechanical properties to support or match the regenerative tissues at the site of implantation. To accomplish this goal, the mechanical properties of cultured scaffold material should be close to those of the surrounding cartilage. At 4 weeks after cultivation, the percentage compression modulus of our chondrocytes-seeded scaffolds to normal rabbit cartilage ranged from 33% to 66%, in terms of scaffold pore size. Investigators have reported the mechanical properties of regenerated cartilage tissue using various kinds of scaffolds.<sup>14,15</sup> Bryant et al.<sup>14</sup> reported that the initial compressive modulus of the photocrosslinked hydrogels based on polyethylene glycol increased from 60 kPa to 500 kPa by increasing the initial macromer concentration. Hoemann et al.<sup>15</sup> showed that the modulus of chondrocytes seeded in agarose and in chitosan gel at 20 days after cultivation was 28.1 kPa and 11.6 kPa, respectively. As shown in the results section, the compression modulus of normal cartilage of rabbits was 3.28 MPa ( $3.280 \times 10^3$  kPa). Although these hydrogels support accumulation of cartilage matrix by chondro-

cytes, the lack of their mechanical properties should be considered. On the other hand, to increase the mechanical properties of cultured implant, 3-D porous scaffolds fabricated from fiber materials have been designed for cartilage tissue engineering.<sup>13,16,17</sup> Woodfield and coauthors<sup>13,17</sup> developed porous scaffolds fabricated with hydrophilic poly(ethylene glycol)-terephthalate (PEGT) and hydrophobic poly(butylene terephthalate) (PBT). They showed that the scaffolds with a 1-mm spacing resulted in a similar dynamic stiffness values compared with bovine and human articular cartilage.<sup>17</sup> Additionally, these scaffolds supported rapid attachment of bovine chondrocytes and cartilage tissue formation following dynamic culture *in vitro*. In the current study, we successfully increased the mechanical properties of scaffolds fabricated from hybrid polymer fibers. Based on the present and previous results, to achieve adequate mechanical strength of scaffolds for cartilage tissue engineering, a promising approach is to design fabricated scaffolds using fibrous materials.

Biocompatible scaffolds for use in cartilage regeneration require at least two characteristics. One is to support cell attachment, proliferation, and ECM production. The other is to provide adequate mechanical strength for regenerated tissue *in vivo*. To our knowledge, most scaffolds developed to date for cartilage regeneration conform to only one of these characteristics. The results obtained here indicate that our novel scaffolds have these favorable biological and mechanical effects on cartilage tissue regeneration *in vitro*. In addition, it was clarified that these effects depend on pore size of the scaffolds. While the scaffold with small pore size (100  $\mu\text{m}$ ) significantly increased the mechanical properties, that with large pore size (400  $\mu\text{m}$ ) significantly enhanced the ECM production by chondrocytes. Several studies have reported that an increased proteoglycans or GAG content of formed cartilage tissue results in improved compressive mechanical properties.<sup>16,18</sup> The compression modulus of our scaffold with 100  $\mu\text{m}$  pore size was comparable to normal articular cartilage of rabbits. However, they significantly decreased at 4 weeks after cultivation. We speculate that the decrease in mechanical strength may be due to mainly measuring the regenerated tissue onto the surface of scaffolds. The other possibility of decrease in mechanical property of the 100  $\mu\text{m}$  pore scaffold after 4 weeks cultivation may be the degradation of fibers. Theoretically, chitosan is not degraded by hydrolysis, but it might be possible that chondrocytes attached to the scaffold material accumulated the factors to dissolve the chitosan. On the other hand, the scaffolds with 400  $\mu\text{m}$  pore size significantly increased the GAG production by chondrocytes. Although a significant alteration was not statistically detected, this increase in the GAG content led to the tendency of enhancing the mechanical proper-

ties of the cultured scaffold. If the scaffold with 400  $\mu\text{m}$  pore size was cultured for a longer period *in vitro* or *in vivo*, an increase in mechanical properties of regenerated tissues on the scaffold may be achieved with enhancing the ECM synthesis by cultured chondrocytes. We, therefore, reasonably conclude that the current scaffold fabricated from the novel hybrid polymer fibers with relatively large pore size (400  $\mu\text{m}$ ) is suited for use in cartilage tissue engineering.

In the current study, we must consider that the results were derived from an *in vitro* experimental model. Therefore, the biocompatibility of the current fibrous material in living joints is still unclear. Several studies have reported the tissue response to various chitosan-based materials.<sup>19–24</sup> In general, these chitosan materials have been observed to evoke a minimal inflammatory or immunological reaction. Suh and Matthew<sup>25</sup> stated that this reaction might play a role in inducing local cell proliferation and ultimately integration of the implanted material with the host tissue. To clinically use chitosan-based materials as a scaffold for cartilage tissue engineering, the immunological reaction during the degradation process of implanted material should be prevented in living joints. An approach for minimizing this reaction is to decrease the amount of artificial material and increase the ECM secreted by chondrocytes. Therefore, we think that the current fibrous material with large pore size, which can enhance the ECM products by cultured chondrocytes, has great potential of becoming an approved scaffold material for cartilage tissue engineering. A future direction of our study will be to clarify these points using animal experimental models.

In conclusion, although we did not observe the biocompatibility of the current fibrous material in living joints, the data derived from this study suggest great promise for the future of the novel fabricated material with relatively large pore size as a scaffold for cartilage regeneration. Additionally, this scaffold showed enhanced mechanical properties, compared with liquid and gel materials. The biological and mechanical advantages presented here will make it possible to apply the current scaffold to relatively wide cartilaginous lesions caused by various joint diseases, including osteoarthritis and rheumatoid arthritis.

The authors thank Mr. Tohru Mitsuno and Mr. Shouzo Miyoshi (General Research Center, Denki Kagaku Kougyo Co. Ltd., Tokyo, Japan) for their excellent technical assistance in fiber preparation.

## References

1. Brittberg M, Lindahl A, Nilsson A, Ohlsson C, Isaksson O, Peterson L. Treatment of deep cartilage defects in the knee

- with autologous chondrocyte transplantation. *N Engl J Med* 1994;331:889-895.
2. Brittberg M, Peterson L, Sjogren-Jansson E, Tallheden T, Lindahl A. Articular cartilage engineering with autologous chondrocyte transplantation. A review of recent developments. *J Bone Joint Surg Am* 2003;85-A(Suppl 3):109-115.
  3. Ochi M, Uchio Y, Kawasaki K, Wakitani S, Iwasa J. Transplantation of cartilage-like tissue made by tissue engineering in the treatment of cartilage defects of the knee. *J Bone Joint Surg Br* 2002;84:571-578.
  4. Brittberg M, Tallheden T, Sjogren-Jansson B, Lindahl A, Peterson L. Autologous chondrocytes used for articular cartilage repair: An update. *Clin Orthop Relat Res* 2001;Oct (391 Suppl):S337-S348.
  5. Hauselmann HJ, Fernandes RJ, Mok SS, Schmid TM, Block JA, Aydelotte MB, Kuettner KE, Thonar, EJ. Phenotypic stability of bovine articular chondrocytes after long-term culture in alginate beads. *J Cell Sci* 1994;107(Part 1):17-27.
  6. Kimura T, Yasui N, Ohsawa S, Ono K. Chondrocytes embedded in collagen gels maintain cartilage phenotype during long-term cultures. *Clin Orthop Relat Res* 1984;186:231-239.
  7. Yamane S, Iwasaki N, Majima T, Punakoshi T, Masuko T, Harada K, Minami A, Monde K, Nishimura S. Feasibility of chitosan-based hyaluronic acid hybrid biomaterial for a novel scaffold in cartilage tissue engineering. *Biomaterials* 2005;26:611-619.
  8. Iwasaki N, Yamane ST, Majima T, Kasahara Y, Minami A, Harada K, Nonaka S, Maekawa N, Tamura H, Tokura S, Shiono M, Monde K, Nishimura S. Feasibility of polysaccharide hybrid materials for scaffolds in cartilage tissue engineering: Evaluation of chondrocyte adhesion to polyion complex fibers prepared from alginate and chitosan. *Biomacromolecules* 2004;5:828-833.
  9. Kim YJ, Sah RL, Doong JY, Grodzinsky, AJ. Fluorometric assay of DNA in cartilage explants using Hoechst 33258. *Anal Biochem* 1988;174:168-176.
  10. Farndale RW, Buttle DJ, Barrett, AJ. Improved quantitation and discrimination of sulphated glycosaminoglycans by use of dimethylmethylene blue. *Biochim Biophys Acta* 1986;883:173-177.
  11. Nehr S, Breinan HA, Ramappa A, Shortkroff S, Young G, Minas T, Sledge CB, Yannas IV, Spector M. Canine chondrocytes seeded in type I and type II collagen implants investigated in vitro. *J Biomed Mater Res* 1997;38:95-104.
  12. Bhardwaj T, Pilliar RM, Grynblas MD, Kandel, RA. Effect of material geometry on cartilaginous tissue formation in vitro. *J Biomed Mater Res* 2001;57:190-199.
  13. Malda J, Woodfield TB, van der Vloot F, Wilson C, Martens DE, Tramper J, van Blitterswijk CA, Riesle J. The effect of PEGT/PBT scaffold architecture on the composition of tissue engineered cartilage. *Biomaterials* 2005;26:63-72.
  14. Bryant SJ, Bender RJ, Durand KL, Anseth, KS. Encapsulating chondrocytes in degrading PEG hydrogels with high modulus: Engineering gel structural changes to facilitate cartilaginous tissue production. *Biotechnol Bioeng* 2004;86:747-755.
  15. Hoemann CD, Sun J, Legare A, McKee MD, Buschmann, MD. Tissue engineering of cartilage using an injectable and adhesive chitosan-based cell-delivery vehicle. *Osteoarthritis Cartilage* 2005;13:318-329.
  16. Chen G, Sato T, Ushida T, Hirochika R, Shirasaki Y, Ochiai N, Tateishi T. The use of a novel PLGA fiber/collagen composite web as a scaffold for engineering of articular cartilage tissue with adjustable thickness. *J Biomed Mater Res A* 2003;67:1170-1180.
  17. Woodfield TB, Malda J, de Wijn J, Peters F, Riesle J, van Blitterswijk, CA. Design of porous scaffolds for cartilage tissue engineering using a three-dimensional fiber-deposition technique. *Biomaterials* 2004;25:4149-4161.
  18. Waldman SD, Grynblas MD, Pilliar RM, Kandel, RA. The use of specific chondrocyte populations to modulate the properties of tissue-engineered cartilage. *J Orthop Res* 2003;21:132-138.
  19. Lu JX, Prudhommeaux F, Meunier A, Sedel L, Guillemin G. Effects of chitosan on rat knee cartilages. *Biomaterials* 1999;20:1937-1944.
  20. Denuziere A, Ferrier D, Damour O, Domard A. Chitosan-chondroitin sulfate and chitosan-hyaluronate polyelectrolyte complexes: Biological properties. *Biomaterials* 1998;19:1275-1285.
  21. Rao SB, Sharma, CP. Use of chitosan as a biomaterial: Studies on its safety and hemostatic potential. *J Biomed Mater Res* 1997;34:21-28.
  22. Muzzarelli, RA. Human enzymatic activities related to the therapeutic administration of chitin derivatives. *Cell Mol Life Sci* 1997;53:131-140.
  23. VandeVord PJ, Matthew HW, DeSilva SP, Mayton L, Wu B, Wooley, PH. Evaluation of the biocompatibility of a chitosan scaffold in mice. *J Biomed Mater Res* 2002;59:585-590.
  24. Tomihata K, Ikada Y. In vitro and in vivo degradation of films of chitin and its deacetylated derivatives. *Biomaterials* 1997;18:567-575.
  25. Suh JK, Matthew, HW. Application of chitosan-based polysaccharide biomaterials in cartilage tissue engineering: A review. *Biomaterials* 2000;21:2589-2598.

## Bone Marrow Stromal Cells Act as Feeder Cells for Tendon Fibroblasts through Soluble Factors

KAZUMI SHIMODE, M.D., NORIMASA IWASAKI, M.D., Ph.D., TOKIFUMI MAJIMA, M.D., Ph.D.,  
TADANAO FUNAKOSHI, M.D., Ph.D., NAOHIRO SAWAGUCHI, M.D., Ph.D.,  
TOMOHIRO ONODERA, M.D., and AKIO MINAMI, M.D., Ph.D.

### ABSTRACT

Feeder effects of bone marrow stromal cells (BMSCs) on tendon fibroblasts were investigated using a co-culture method for the application of ligament or tendon tissue engineering and cell therapy. BMSCs had significant effects on enhancing cell proliferation, the ability of cells to migrate, and cell adhesivity but little effect on the extracellular matrix (ECM) synthesis of tendon fibroblasts without cell-cell contact. Furthermore, the conditioned medium from BMSCs, despite the existence of fibroblasts, significantly increased the number of fibroblasts. Based on these results, the mechanism of the feeder effects is considered to be a certain signal of soluble factors from BMSCs to the fibroblasts. Comparative proteome analysis of the conditioned medium from co-culture of fibroblasts and BMSCs revealed less expression of plasminogen, which showed inhibitory effects on fibroblast proliferation. With regard to the relationships between plasminogen and BMSCs in the co-culture system, we speculate that BMSCs allow resolution of plasminogen or its cleavage activity in the medium via some mechanism.

### INTRODUCTION

**B**ONE MARROW STROMAL CELLS (BMSCs) are pluripotent progenitor cells that have the ability to differentiate into various kinds of musculoskeletal tissue cells.<sup>1</sup> Therefore, these cells have been used as an alternative source of tissue-derived mature cells for musculoskeletal tissue engineering.<sup>2,3</sup> On the other hand, recent studies have reported that BMSCs act as feeder cells for some types of cells *in vitro*.<sup>4-8</sup>

Tendon and ligament injuries frequently occur in daily activities. Most of these injuries heal naturally in a living body. The process of tendon and ligament healing is a complex one. This process takes place in four phases: hemorrhage, inflammation, proliferation, and remodeling or maturation. In the inflammatory phase, various kinds of cells, including fibroblasts, platelets, white blood cells, and BMSCs, enter the wounded area. These cells themselves and cellular inter-

actions play a crucial role in the healing process.<sup>9-11</sup> In particular, BMSCs contribute to the process of tendon and ligament healing.<sup>12,13</sup> There are at least two possible ways that BMSCs contribute to this healing process. One possibility is that BMSCs themselves differentiate into fibroblasts at the injury site. The other is that BMSCs have a regulative effect on enhancing the biological behaviors of fibroblasts via cell-cell contact or soluble factors. Several studies have clarified that cell-cell contact, called cell fusion, is essential for BMSCs to repair myocardial infarction<sup>14</sup> and damaged liver tissue.<sup>15</sup> It is also recognized that the soluble factors secreted by BMSCs induce neural stem cell differentiation.<sup>16</sup> However, little attention has been given to the interactions between tendon or ligament fibroblasts and BMSCs. Much about the role of these interactions remains to be understood.

In the current study, we focused on the effects of soluble factors of BMSCs on the biological behaviors of fibroblasts.

We hypothesized that BMSCs combined with tendon fibroblasts could enhance the cellular activities of fibroblasts via some soluble factors. To test this hypothesis, rat tendon fibroblasts were co-cultured with rat BMSCs in the micro-porous membrane-separated co-culture systems. The main objective of the current study was to determine the feeder effects of BMSCs on the tendon fibroblasts in terms of proliferation, the synthesis of extracellular matrices (ECMs), the ability to migrate, and cell adhesivity. Then we attempted to reveal the specific soluble factors significantly affecting the fibroblast behaviors. The data obtained here will be beneficial to the use of BMSCs as feeder cells for ligament or tendon tissue engineering and cell therapy.

## MATERIALS AND METHODS

### Study protocol

Figure 1 shows the flow chart of the current study protocol. First, we examined the feeder effects of BMSCs on

the cultured tendon fibroblasts (membrane-separated co-culture study). Next, we attempted to explore the specific soluble factors affecting the behavior of BMSCs (conditioned medium study).

### Fibroblast isolation

Fibroblasts were isolated from the Achilles tendon substance of 6-week-old WKAH rats under sterile conditions, as described by Nagineni *et al.*<sup>17</sup> To avoid contamination, the peritendinous tissues were carefully removed. Two weeks after culturing, the explanted pieces of Achilles tendon were discarded, and the outgrown cells were removed for subculture. The fibroblasts were used at the fourth and seventh passages in this study.

### BMSC isolation

BMSCs were isolated from WKAH rats using the following procedure. Bone marrow cells were obtained from the femurs and tibias by flushing the shaft using a syringe

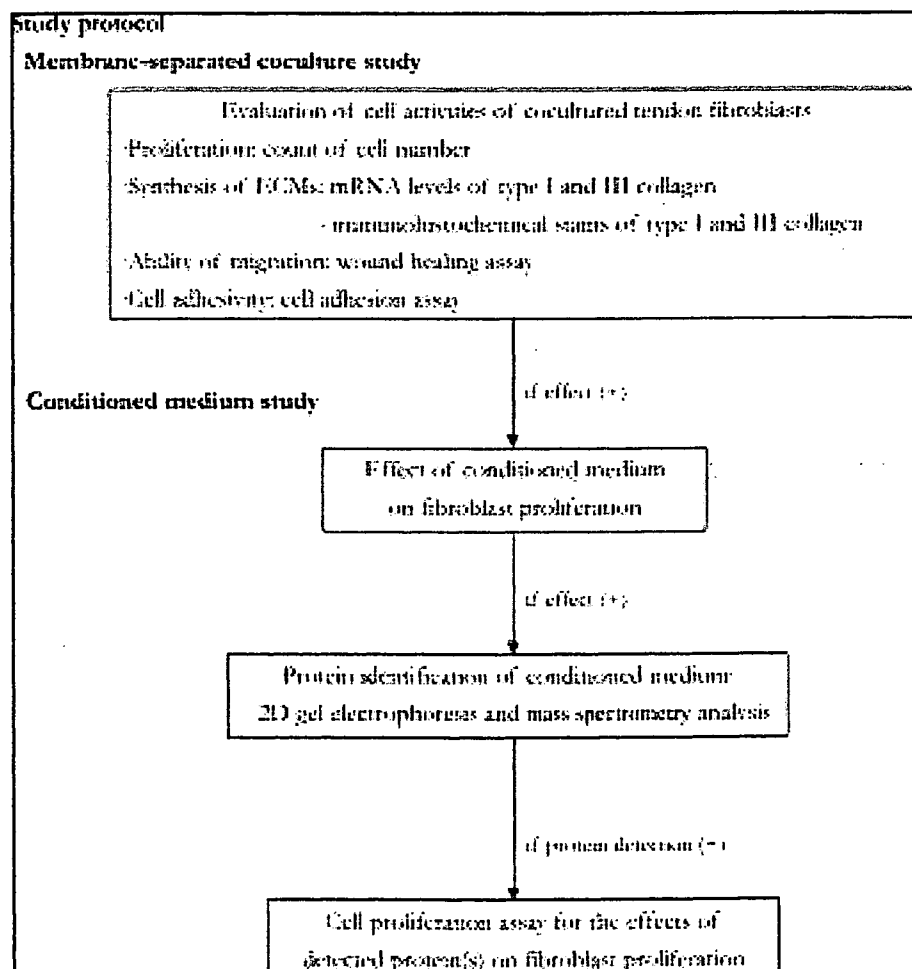


FIG. 1. Flow chart of the study protocol. ECM, extracellular matrix; mRNA, messenger ribonucleic acid; 2D, 2-dimensional.

## BMSCs ACT AS FEEDER CELLS

with a 22-gauge needle under sterile conditions. The cells were disaggregated by gentle pipetting several times and passed through a 70  $\mu\text{m}$  cell strainer (BD Biosciences, San Jose, CA) to remove remaining clumps of tissue. Finally, the collected cells were seeded on culture dishes, and the adhesive cells were used as BMSCs. The BMSCs at the second passage were used for further investigations.

### General culture condition

The culture medium used here was Dulbecco's modified Eagle's medium (D5796, Sigma Chemical Co., St. Louis, MO) with or without 10% fetal calf serum (FCS, 812072, Invitrogen Corp., Carlsbad, CA), 10  $\mu\text{L}/\text{mL}$  penicillin, streptomycin, and Fungizone (17-745H, Biowhittaker, Walkersville, MD). The cells were incubated at 37°C in a humidified atmosphere of 95% air and 5% carbon dioxide. Cell counts were performed after trypsinization using a hemocytometer. All procedures involving animals were according to the established ethical guidelines approved by the local animal care committee.

### Cell proliferation of co-cultured fibroblasts.

Fibroblasts ( $1 \times 10^4$  cells) were seeded in BD Falcon Multiwell Insert Systems with a microporous membrane (6 wells, pore diameter 1  $\mu\text{m}$ , BD Biosciences) with  $5 \times 10^5$  feeder cells of BMSCs (co-culture group) or fibroblasts (control group). The pore diameter of 1  $\mu\text{m}$  prohibits cell transportation across the membrane. The culture medium with FCS was filled with 4 mL in each experimental group and changed twice a week. The number of fibroblasts was counted at day 3, 7, 10, and 14 after seeding in each experimental group ( $n = 10$  at each time period).

### ECM synthesis of co-cultured fibroblasts.

To detect messenger ribonucleic acid (mRNA) expression of type I and type III collagen in the co-cultured fibroblasts, total mRNA was extracted from the fibroblasts at day 7 after seeding in each group according to the TRIzol Reagent protocol (Invitrogen Corp.). For this analysis, we needed the samples before the cultured fibroblasts reached confluence. Therefore, the samples at day 7 were used. Quantitative real-time reverse transcription polymerase chain reaction (RT-PCR) was performed using the SYBR green PCR kit in Opticon II (Bio Rad, Hercules, CA) with gene-specific primer of type I and type III collagen designed using OLIGO (Molecular Biology Insights, Cascade, CO). Average threshold cycle (ct) values of type I and type III collagen were normalized to those of glyceraldehyde-3-phosphate dehydrogenase (GAPDH) transcript levels. Primer sequences were as follows: type I collagen; forward primer 5'TCAAGATGG TGGCCGTTAC3', reverse primer 5'CTGCGGATGTTCTC AATCTG3'; type III collagen, forward primer 5'GGCAAG GGTGATCGTGGTG3', reverse primer 5'GACCAGCAGG ACCCGTTTCT3'; GAPDH, forward primer 5'CAACCAC

CTGTTGCTGTA3', reverse primer 5'TATGATGACAT CAAGAAGCTGG3'. Immunohistochemical stains of fibroblasts were performed with anti-type I collagen (LSL-LB-1102, Cosmo Bio, Tokyo, Japan) and anti-type III collagen (LSL-LB-1387, Cosmo Bio). For this evaluation, the samples at day 14 were used.

### Wound healing assay

To assess the migratory ability of co-cultured fibroblasts, *in vitro* wound-healing assay was performed according to the protocol of Nagineni *et al.*<sup>17</sup> with some modifications. Briefly, fibroblasts were seeded at the density of  $1 \times 10^5$  cells/well in BD Falcon Multiwell plates (12 wells, BD Biosciences) after 7 days of co-culture in each group. At the time of confluence, the medium was removed from the culture dish and replaced with serum-free medium. After 24 h, a uniform wound of approximately 800  $\mu\text{m}$  in width was created in the mid-portion of the culture dish by scraping with a sterile yellow pipette tip. Then, the culture dish was filled with serum-free medium after washing 3 times with PBS. At 3, 6, 12, 24, 48, and 72 h after the wound was created, the distance of migration from the wound edge was calculated using a microscopic photograph ( $n = 10$ ).

### Cell adhesion assay

To test the cell adhesivity of co-cultured fibroblasts, a cell adhesion assay using WST-8 (Dojindo Laboratories, Kumamoto, Japan) was performed according to the method described previously.<sup>18</sup> Ninety-six-well plates (Falcon Microtest Plates, BD Biosciences) were used. Nonspecific binding sites were blocked by incubating the plates with 100  $\mu\text{L}$  of 2% bovine serum albumin for 1 h at 37°C. Then the wells were washed 3 times with PBS. After 7 days of co-culture, fibroblasts ( $1 \times 10^5$  cells/well) from each group were added to the wells with 100  $\mu\text{L}$  of serum-free medium and incubated for 1 h at 37°C. The unbound cells were removed by gently rinsing the wells 3 times with PBS. Then, 100  $\mu\text{L}$  of serum-free medium and 10  $\mu\text{L}$  of the working solution of WST-8 were added to each well that had cells in it. The mixtures were incubated for an additional 4 h. The optic density (OD) of each well was measured at 450 nm using a Microplate Reader (Benchmark Plus, Bio Rad) against the reference absorbance of 600 nm.

### Conditioned medium culture

To confirm the effects of soluble factors from BMSCs on the proliferation of tendon fibroblasts, culture supernatants (conditioned medium) were collected from the co-culture and the control groups. Furthermore, to clarify the necessity of cross-talk between fibroblasts and BMSCs to affect the soluble factors, the culture supernatants were also collected from BMSCs ( $5 \times 10^5$  cells) of WKAH rats without feeding cells of fibroblasts (BMSC-only group) with 2 mL of culture medium with FCS for 14 days. The conditioned medium

was collected when the medium was changed during the culture period. Fibroblasts ( $1 \times 10^4$  cells) were cultured in 2 mL of each conditioned medium without feeder cells in Falcon Multiwell plates (6 wells, BD Biosciences). The number of fibroblasts was counted at day 3, 7, 10, and 14 after seeding in all experimental groups ( $n = 6$  at each time period).

#### Two-dimensional gel electrophoresis and mass spectrometry analysis for protein identification

To detect some proteins as soluble factors, a comparative 2-dimensional (2D) gel electrophoresis and mass spectrometry (MS) analysis using the conditioned medium from the co-culture and the control groups were performed, according to the method described previously,<sup>19,20</sup> at Hitachi Science Systems Ltd. (Ibaraki, Japan). Before the separation and analysis of the proteins using 2D sodium dodecyl sulfate-polyacrylamide gel electrophoresis (SDS-PAGE), the proteins of the conditioned medium were concentrated using a Centrplus centrifugal filter device YM-10 (10000-MW, cut off; Millipore, Bedford, MA). Albumin and immunoglobulin G (IgG) were removed from the centrifuged proteins using a ProteoExtract Albumin/IgG removal kit (Calbiochem, EMD Biosciences, Darmstadt, Germany) and Multiple Affinity Removal System Kit (Agilent Technologies, Palo Alto, CA). Then, the 2D SDS-PAGE was performed on gradient gel (8–16%, 17 cm, Bio Rad) using Protean II xi cell (Bio Rad) after precipitation using trichloroacetic acid to remove electrolytes. The spots were visualized by silver staining using a SilverQuest Silver Staining Kit (Invitrogen Corp.). The 2D images were analyzed and compared using PDQuest (Bio Rad) and optical confirmation. The resulting peptide samples were analyzed using time-of-flight MS (Applied Biosystems, Foster, CA) after being spotted on a MALDI plate and co-crystallized with 2, 5-dihydroxybenzoic acid. Mass spectra were recorded on a MALDI-TOF instrument (oMALDI-Qq-TOF MS/MS, Applied Biosystems).

#### Cell proliferation assay for the effects of detected protein on fibroblast proliferation

Cell proliferation assay was performed to confirm the effect of the protein(s) detected in the 2D gel electrophoresis. In this assay, we used WST-8 to quantify the number of fibroblasts. In brief, fibroblasts were seeded on 96 well plates (Falcon Microtest Plates, BD Biosciences) at  $3 \times 10^3$  cells/well with increasing concentration of the detected protein.<sup>21</sup> After 6, 12, 24, 48, and 72 h incubation, cell number was quantified using WST-8 according to the protocol mentioned in the cell adhesion assay section ( $n = 5$  at each time period).

#### Statistical analysis

All data were represented as means  $\pm$  standard errors. Significant differences between the groups were assessed

using unpaired t-test or one-way analysis of variance and Fischer's protected least significant difference post hoc tests. *P*-values of less than 0.05 were considered significant.

## RESULTS

After 3 days of co-culture, the number of fibroblasts in the co-culture group increased significantly more with time than did those in the control group ( $0.19 \pm 0.01 \times 10^5$  vs.  $0.05 \pm 0.05 \times 10^5$  cells at day 3,  $2.62 \pm 0.17 \times 10^5$  vs.  $0.72 \pm 0.26 \times 10^5$  cells at day 7,  $5.40 \pm 0.66 \times 10^5$  vs.  $2.06 \pm 0.17 \times 10^5$  cells at day 10, and  $6.92 \pm 0.85 \times 10^5$  vs.  $2.86 \pm 0.27 \times 10^5$  cells at day 14; Fig. 2). The cell density of fibroblasts in the co-culture group was higher than that in the control group, and it reached confluence at 10 days of co-culture in the co-culture group, but not in the control group.

Regarding mRNA levels of type I and type III collagen synthesized by fibroblasts, no statistically significant differences in the values were found between the co-culture and control groups ( $5.42 \pm 0.38$  vs.  $5.13 \pm 0.41$  for type I collagen,  $0.62 \pm 0.09$  vs.  $0.50 \pm 0.05$  for type I collagen). Immunohistochemical evaluation revealed the type I and type III collagen products in both groups (Fig. 3).

The wound healing assay showed that the fibroblasts of the co-culture group had significantly better ability of migration than the fibroblasts of the control group at each time point from 6 to 72 h after *in vitro* wounding ( $62.5 \pm 3.2$  vs.  $36.1 \pm 2.2 \mu\text{m}$  at 6 h,  $101 \pm 3.9$  vs.  $59.0 \pm 3.7 \mu\text{m}$  at 12 h,  $154 \pm 5.2$  vs.  $78.1 \pm 6.2 \mu\text{m}$  at 24 h,  $364 \pm 5.2$  vs.  $185 \pm 11.4 \mu\text{m}$  at 48 h, and  $393 \pm 20.1$  vs.  $226 \pm 15.9 \mu\text{m}$  at 72 h; Fig. 4 and Fig. 5). In the cell adhesion assay, BMSCs increased the cellular adhesivity of co-cultured fibroblasts significantly, from  $1.16 \pm 0.09$  to  $1.81 \pm 0.07$  (OD,  $p < 0.05$ ).

The results mentioned above suggested the feeder effects of BMSCs on tendon fibroblasts via soluble factors. To confirm this point, we then cultured tendon fibroblasts with

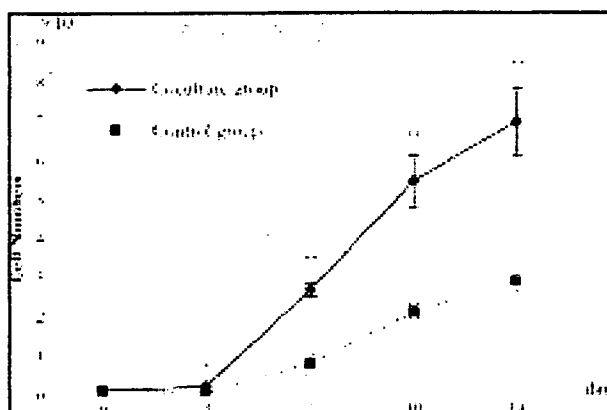


FIG. 2. Significant increase in cell number of co-cultured fibroblasts after being seeded in micro-porous membrane-separated co-culture systems. \* $p < 0.05$ , \*\* $p < 0.01$ .

BMSCs ACT AS FEEDER CELLS

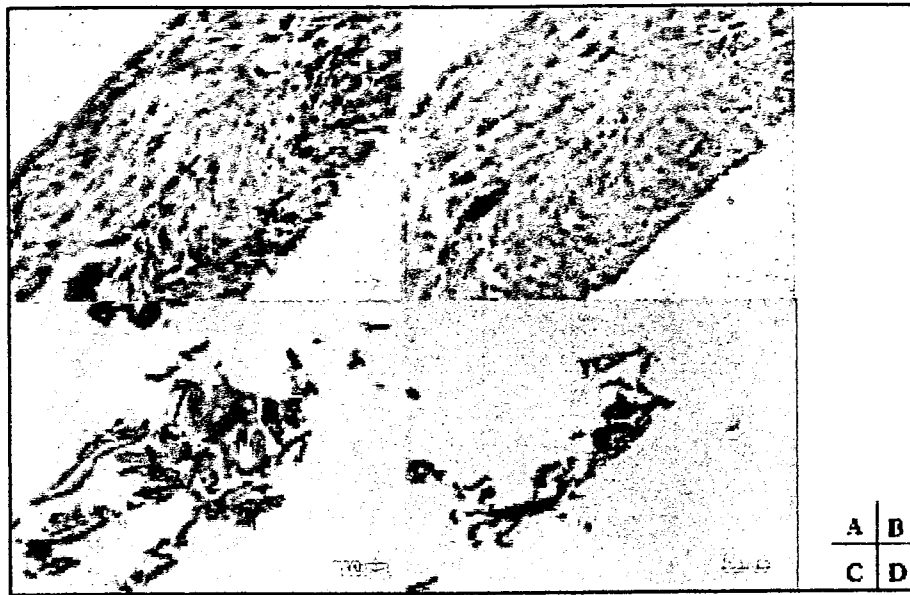


FIG. 3. Immunohistochemistry of scraped fibroblasts in the co-culture group for type I collagen (A), in the co-culture group for type III collagen (B), in the control group for type I collagen (C), and in the control group for type III collagen (D) at 14 days after coculture. There are apparently more extracellular matrix products in the co-culture group than in the control group. Scale bars: 50  $\mu$ m.

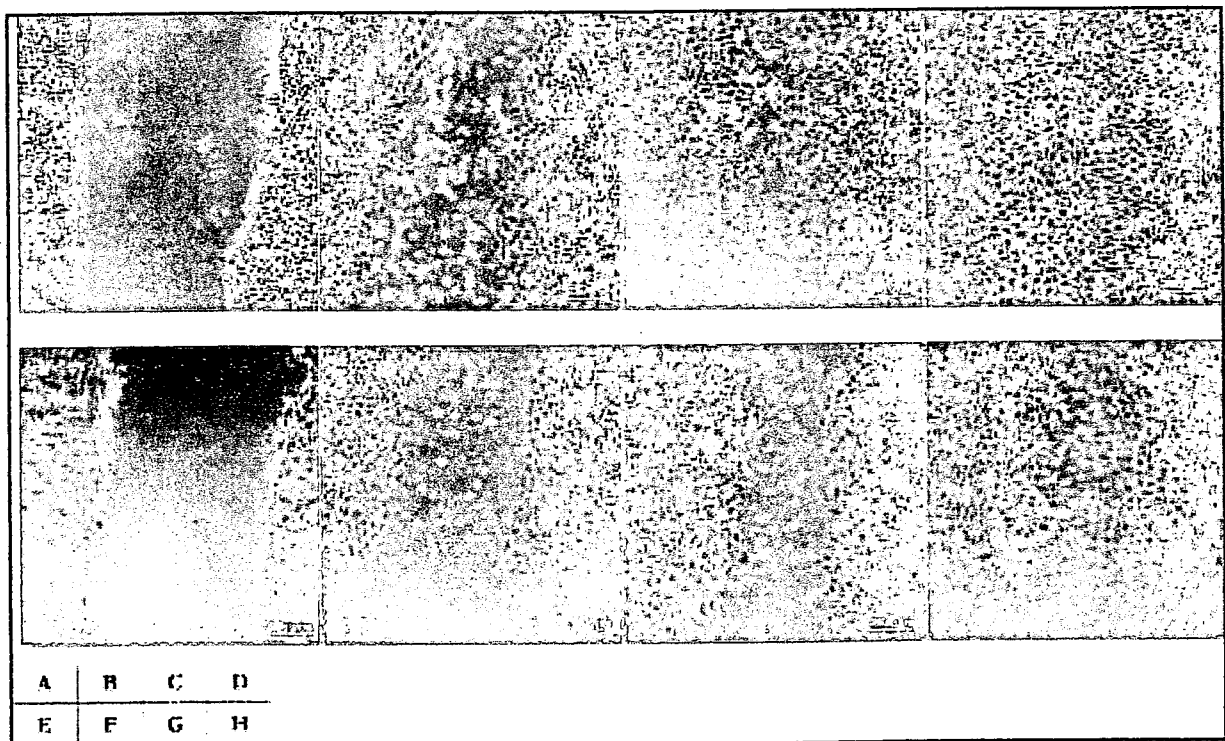


FIG. 4. Microscopic appearance of wound healing assay (A-D; fibroblasts cocultured with bone marrow stromal cells, E-H; control: 0, 24, 48, and 72 h after *in vitro* wounding). Scale bars: 200  $\mu$ m.



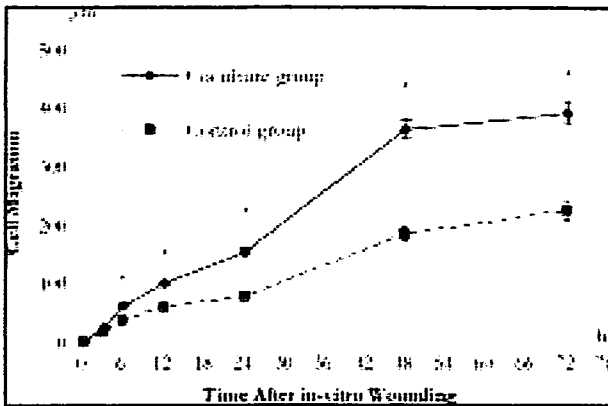


FIG. 5. The distance of migration of co-cultured fibroblasts calculated from microscopic photography. The fibroblasts co-cultured with bone marrow stromal cells show superior ability of migration.  $*p < 0.01$ .

the conditioned medium from the co-culture and the control groups. The number of fibroblasts cultured with conditioned medium from the co-culture group increased significantly more than that of the control group at 7 days after culture ( $1.25 \pm 0.08 \times 10^5$  vs.  $0.40 \pm 0.05 \times 10^5$  cells at day 7,  $3.21 \pm 0.51 \times 10^5$  vs.  $0.63 \pm 0.07 \times 10^5$  cells at day 10, and  $6.29 \pm 1.75 \times 10^5$  vs.  $1.00 \pm 0.14 \times 10^5$  cells at day 14; Fig. 6). Furthermore, we then cultured tendon fibroblasts with the conditioned medium from the culture of BMSCs alone (BMSC-only group). The number of fibroblasts cultured with this conditioned medium was higher than that of the control group after 7 days of culture ( $1.05 \pm 0.05 \times 10^5$  vs.  $0.40 \pm 0.05 \times 10^5$  cells at day 7,  $2.90 \pm 0.50 \times 10^5$  vs.  $0.63 \pm 0.07 \times 10^5$  cells at day 10, and  $5.05 \pm 1.67 \times 10^5$  vs.  $1.00 \pm 0.14 \times 10^5$  cells at day 14; Fig. 6). We did not observe a significant difference in the cell number of fibro-

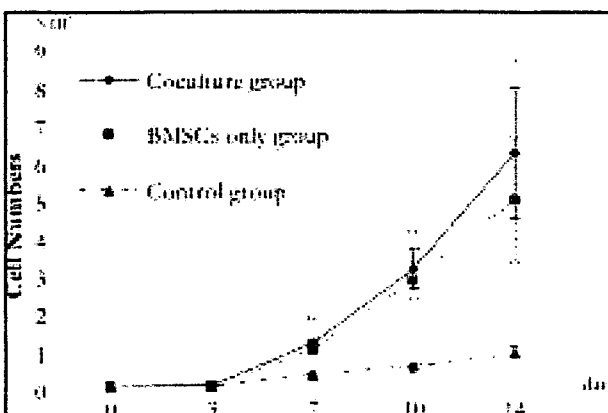


FIG. 6. Increase in cell number of fibroblasts cultured with conditioned medium after being seeded. The fibroblasts cultured with conditioned medium from the coculture and bone marrow stromal cells (BMSCs) only show greater levels of proliferation.  $*p < 0.05$ ,  $**p < 0.01$ .

blasts between the co-culture group and the BMSC-only group. These results indicate that the existence of fibroblasts was unnecessary for the feeder effects of BMSCs.

To detect any soluble factors contributing to these feeder effects, comparative proteome analysis was performed with conditioned medium from the co-culture group and the control group. Figure 7 shows the position of the proteins included in conditioned medium of the 2 groups on the 2D gels after 2D SDS-PAGE and silver staining. There were 6 spots of proteins, which showed differences in size between the 2 groups. Among them, 4 spots showed a greater difference (spots 2, 3, 4, and 5), and MS analysis was consequently performed on these proteins. Mass spectrometry analysis revealed spot 2 and spot 4 to be transthyretin (prealbumin), spot 3 to be plasminogen, and spot 5 to be hear-keratin. Of these proteins, we selected plasminogen, which showed greater expression in the control, as a candidate to affect the fibroblast proliferation. To test the effect of plasminogen on fibroblast proliferation, this protein was added to the medium with increasing concentration from 0 nM to 200 nM. The results showed that there were significant differences between the three groups at 24, 48, and 72 h after cultivation. These results indicate that plasminogen significantly inhibits fibroblast proliferation with dose and time dependency (Fig. 8).

## DISCUSSION

The main purpose of this study was to determine the feeder effects of BMSCs on the tendon fibroblasts in a co-culture system. The results obtained here suggest that BMSCs have feeder effects on the proliferation, the ability of migration, and the cell adhesivity of rat tendon fibroblasts in an *in vitro* culture system. There have been numerous studies on cell-cell interactions with the use of co-culture systems.<sup>4-8,16,22-25</sup> Many of these studies have demonstrated that BMSCs work as cell mediators, which influence proliferation, viability, and the differentiation of various types of cells *in vitro*.<sup>4-8,16,22-25</sup> There are two explanations of the mechanism of these effects, including via cell-cell contact or some soluble factors. In the current study, we found that fibroblasts co-cultured with BMSCs led to enhanced fibroblast activity and that the conditioned mediums from BMSCs alone and from BMSCs co-cultured with fibroblasts increased the number of fibroblasts significantly. Based on these results, the feeder effects clarified here are considered to be certain signals of soluble factors from BMSCs to the fibroblasts without cross-talk between these two types of cells.

The current study indicates that plasminogen, as a significantly detected protein in the control medium, has inhibitory effects on the proliferation of co-cultured fibroblasts. Although several studies have detected the specific soluble factors from BMSCs for various kinds of cells, little attention has been given to this point in terms of tendon fibroblasts.

## BMSCs ACT AS FEEDER CELLS

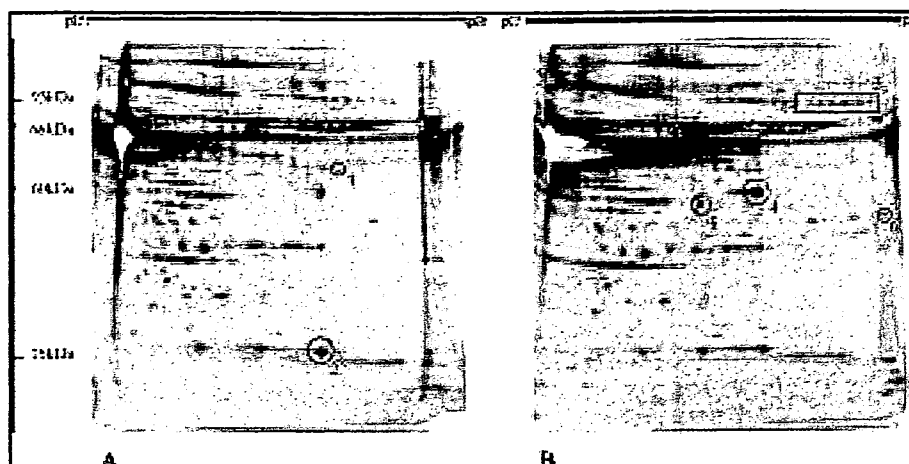


**FIG. 7.** The position of the proteins included in the conditioned medium of the co-culture group (A) and the control group (B) on the 2-dimensional (2D) gels after 2D sodium dodecyl sulfate-polyacrylamide gel electrophoresis and silver staining.

To our knowledge, this is the first study to clarify the feeder effects of BMSCs on tendon fibroblasts and to detect the specific soluble factors affecting their cellular activities. We detected plasminogen not from the conditioned medium from BMSCs but from the control medium without BMSCs. Although plasminogen itself is thought to be an inactive protein, it has been recognized that angiostatin (kringle 1–4) and kringle 5, the enzymatic cleavages of plasminogen, have potential as endogenous inhibitors of some types of cells, including endothelial cells and tumor cells.<sup>19,21,26–29</sup> It is thought that the mechanism of the inhibitory effect of these proteins induces apoptosis in target cells.<sup>19,28</sup> The current study also clarified that plasminogen inhibited the proliferation of tendon fibroblasts. On the other hand, it has also been reported that ligament fibroblasts express plasminogen

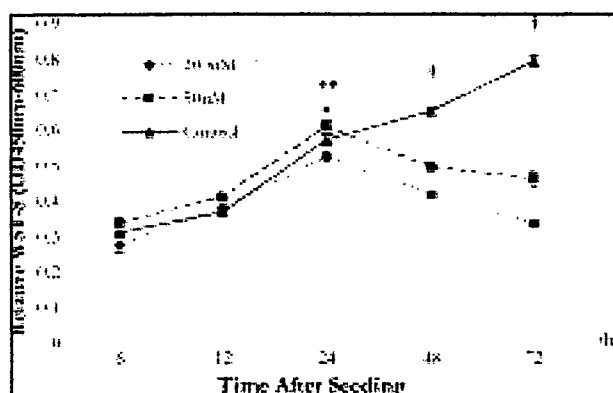


**FIG. 8.** Cell proliferation assay using WST-8 with the addition of increasing concentrations of plasminogen to the culture medium. Plasminogen shows the inhibitory effect on fibroblast proliferation with dose and time dependency. \* $p < 0.05$ , 200 nM vs. control; \*\* $p < 0.01$ , 200 nM vs. 50 nM; † $p < 0.01$ , 200 nM vs. 50 nM vs. control. OD, outer diameter.

activators, an enzyme capable of proteolyzing matrix molecules, and plasminogen activator inhibitors and that these enzymes contribute to a more anabolic environment in case of ligament healing.<sup>30</sup> There is a possibility that these enzymes alter the plasminogen activity and its ability to influence fibroblast behavior in this study. Based on this, we speculate that BMSCs allow resolution of plasminogen or its cleavage activity in the medium via some mechanism. Further study will be needed to clarify this point.

Stem cells play an important role in repairing injured tissues in living bodies. BMSCs are one of the stem cells most capable of repairing injured tendon and ligament.<sup>12,13</sup> Although the detailed effects of BMSCs on the healing process of these tissues are still unclear, there are at least two possibilities of their effects on this process. One is that BMSCs themselves differentiate into fibroblasts at the injury site. Watanabe *et al.* proposed the possibility that BMSCs differentiated into ligament fibroblasts at the site of injury in rats.<sup>12</sup> Other studies showed that BMSCs expressed several fibroblastic markers in tissue-engineered ligament<sup>2</sup> and skin wound lesions.<sup>31–34</sup> The other possibility is a regulative effect of BMSCs on enhancing the biological behavior of fibroblasts via cell–cell contact or soluble factors. To our knowledge, few attempts have been made to confirm such observation, especially in relation to tendons and ligaments. The current study suggests that there is a possibility of positive effects of BMSCs on the *in vivo* healing process of tendons and ligaments through enhanced fibroblast activities.

In tissue-engineering techniques, tissue regeneration is achieved by culturing isolated cells on 3-dimensional scaffolds to develop biological substitutes. For successful tissue regeneration, it is important to increase the number of isolated cells. To achieve this, the addition of cytokines or growth factors, including vascular endothelial growth factor, insulin-like growth factor, platelet-derived growth factor, basic fibroblast growth factor, and transforming growth

factor -beta, to culture medium has been attempted.<sup>35</sup> The application of these proteins has been considered to be the most effective strategy for increasing the number of cells. However, it is doubtful whether the cost-ineffective application of cytokines or growth factors, which has a possibility of leading to the onset of malignancy,<sup>36</sup> will be accepted as a clinical strategy. Based on the results obtained here, we may reasonably conclude that using BMSCs as feeder cells in a co-culture system with tendon fibroblasts is a promising alternative to the application of cytokines or growth factors.

In this study, we must consider the existence of other proteins affecting the fibroblast behavior in the current co-culture system. To clarify the mechanism of feeder effects of BMSCs on various kinds of cells, several studies have attempted to detect proteins as soluble factors. Gupta *et al.* suggested that interleukin-6 and granulocyte-colony stimulating factor produced by BMSCs increased the colony-stimulating activity of hematopoietic stem cells.<sup>4</sup> Nishi *et al.* concluded that granulocyte-colony stimulating factor and stem cell factor were the crucial factors in the culture of primitive hematopoietic cells supported by BMSCs.<sup>5</sup> Yamamoto *et al.* reported that a significant increase of transforming growth factor-beta1, insulin-like growth factor-1, epidermal growth factor, and platelet-derived growth factor was found in co-culture medium of nucleus pulposus cells and BMSCs.<sup>7</sup> We believe that the difference in the detected factors may result from the condition of the culture medium, the number of feeder cells, and the analytical method. Specially, no previous studies have applied gel electrophoresis and MS analysis, used in the current study, to protein identification in co-culture systems. Future studies will be performed to detect other soluble factors with feeder effects on ligament fibroblasts using more precise culture systems and analytical tools.

In conclusion, we have demonstrated the feeder effects of BMSCs on tendon fibroblasts in terms of cellular proliferation, ability to migrate, and cell adhesivity through the soluble factors, with use of an *in vitro* co-culture technique. The proteome analysis revealed that the plasminogen, which was detected from the conditioned medium without BMSCs, had inhibitory effects on fibroblast proliferation. Based on the results obtained, we may reasonably conclude that the feeder effects of BMSCs in the current co-culture system result from expending plasminogen in culture medium using some mechanism. The current co-culture system using BMSCs will be considered for application for tendon and ligament tissue engineering or cell therapy for severe injuries of these tissues.

#### ACKNOWLEDGMENTS

This work was supported by a Grant-in-Aid for Science Research from the Ministry of Education, Culture, Sports, Science and Technology (B-1539044) and a Grant-in-Aid

for New Energy and Industrial Technology Development Organization (03A04002a).

#### REFERENCES

- Pittenger, M.F., Mackay, A.M., Beck, S.C., Jaiswal, R.K., Douglas, R., Mosca, J.D., Moorman, M.A., Simonetti, D.W., Craig, S., and Marshak, D.R. Multilineage potential of adult human mesenchymal stem cells. *Science* **284**, 143, 1999.
- Altman, G.H., Horan, R.L., Martin, I., Farhadi, J., Stark, P.R., Volloch, V., Richmond, J.C., Vunjak-Novakovic, G., and Kaplan, D.L. Cell differentiation by mechanical stress. *Faseb J* **16**, 270, 2002.
- Ponticciello, M.S., Schinagl, R.M., Kadiyala, S., and Barry, F.P. Gelatin-based resorbable sponge as a carrier matrix for human mesenchymal stem cells in cartilage regeneration therapy. *J Biomed Mater Res* **52**, 246, 2000.
- Gupta, P., Blazar, B.R., Gupta, K., and Verfaillie, C.M. Human CD34(+) bone marrow cells regulate stromal production of interleukin-6 and granulocyte colony-stimulating factor and increase the colony-stimulating activity of stroma. *Blood* **91**, 3724, 1998.
- Nishi, N., Ishikawa, R., Inoue, H., Nishikawa, M., Kakeda, M., Yoneya, T., Tsumura, H., Ohashi, H., Yamaguchi, Y., Motoki, K., Sudo, T., and Mori, K.J. Granulocyte-colony stimulating factor and stem cell factor are the crucial factors in long-term culture of human primitive hematopoietic cells supported by a murine stromal cell line. *Exp Hematol* **24**, 1312, 1996.
- Hombauer, H., and Minguell, J.J. Selective interactions between epithelial tumour cells and bone marrow mesenchymal stem cells. *Br J Cancer* **82**, 1290, 2000.
- Yamamoto, Y., Mochida, J., Sakai, D., Nakai, T., Nishimura, K., Kawada, H., and Hotta, T. Upregulation of the viability of nucleus pulposus cells by bone marrow-derived stromal cells: significance of direct cell-to-cell contact in coculture system. *Spine* **29**, 1508, 2004.
- Minges Wols, H.A., Underhill, G.H., Kansas, G.S., and Witte, P.L. The role of bone marrow-derived stromal cells in the maintenance of plasma cell longevity. *J Immunol* **169**, 4213, 2002.
- Woo, S.L., Hildebrand, K., Watanabe, N., Fenwick, J.A., Papageorgiou, C.D., and Wang, J.H. Tissue engineering of ligament and tendon healing. *Clin Orthop Relat Res* **S312**, 1999.
- Ross, R. The fibroblast and wound repair. *Biol Rev Camb Philos Soc* **43**, 51, 1968.
- Andriacchi, T., Sabiston, P., DeHaven, K., Dahners, L., Woo, S.L., Frank, C., Oakes, B., Brand, R., and Lewis, J. Ligament: injury and repair. In: Woo, S.L., and Buckwalter, J.A., eds. *Injury and Repair of the Musculoskeletal Soft Tissues*. Rosemont, IL: American Academy of Orthopaedic Surgeons. 1988, pp. 103-28.
- Watanabe, N., Woo, S.L., Papageorgiou, C., Celechovsky, C., and Takai, S. Fate of donor bone marrow cells in medial collateral ligament after simulated autologous transplantation. *Microsc Res Tech* **58**, 39, 2002.
- Young, R.G., Butler, D.L., Weber, W., Caplan, A.I., Gordon, S.L., and Fink, D.J. Use of mesenchymal stem cells in a collagen matrix for Achilles tendon repair. *J Orthop Res* **16**, 406, 1998.

## BMSCs ACT AS FEEDER CELLS

14. Yoon, Y.S., Wecker, A., Heyd, L., Park, J.S., Tkebuchava, T., Kusano, K., Hanley, A., Scadova, H., Qin, G., Cha, D.H., Johnson, K.L., Aikawa, R., Asahara, T., and Losordo, D.W. Clonally expanded novel multipotent stem cells from human bone marrow regenerate myocardium after myocardial infarction. *J Clin Invest* **115**, 326, 2005.
15. Vassilopoulos, G., Wang, P.R., and Russell, D.W. Transplanted bone marrow regenerates liver by cell fusion. *Nature* **422**, 901, 2003.
16. Lou, S., Gu, P., Chen, F., He, C., Wang, M., and Lu, C. The effect of bone marrow stromal cells on neuronal differentiation of mesencephalic neural stem cells in Sprague-Dawley rats. *Brain Res* **968**, 114, 2003.
17. Nagineni, C.N., Amiel, D., Green, M.H., Berchuck, M., and Akeson, W.H. Characterization of the intrinsic properties of the anterior cruciate and medial collateral ligament cells: an in vitro cell culture study. *J Orthop Res* **10**, 465, 1992.
18. Riss, T. Comparison of attachment factors using the CellTiter 96TM Assay. *Promega Notes Magazine*, 1992, pp. 18–22.
19. Lucas, R., Holmgren, L., Garcia, I., Jimenez, B., Mandriota, S.J., Borlat, F., Sim, B.K., Wu, Z., Grau, G.E., Shing, Y., Soff, G.A., Bouck, N., and Pepper, M.S. Multiple forms of angiostatin induce apoptosis in endothelial cells. *Blood* **92**, 4730, 1998.
20. Shevchenko, A., Wilm, M., Vorm, O., and Mann, M. Mass spectrometric sequencing of proteins silver-stained polyacrylamide gels. *Anal Chem* **68**, 850, 1996.
21. Meneses, P.I., Abrey, L.E., Hajjar, K.A., Gultekin, S.H., Duvoisin, R.M., Berns, K.I., and Rosenfeld, M.R. Simplified production of a recombinant human angiostatin derivative that suppresses intracerebral glial tumor growth. *Clin Cancer Res* **5**, 3689, 1999.
22. Gerstenfeld, L.C., Cruceta, J., Shea, C.M., Sampath, K., Barnes, G.L., and Einhorn, T.A. Chondrocytes provide morphogenic signals that selectively induce osteogenic differentiation of mesenchymal stem cells. *J Bone Miner Res* **17**, 221, 2002.
23. Aggarwal, S., and Pittenger, M.F. Human mesenchymal stem cells modulate allogeneic immune cell responses. *Blood* **105**, 1815, 2005.
24. Jiang, X.X., Zhang, Y., Liu, B., Zhang, S.X., Wu, Y., Yu, X.D., and Mao, N. Human mesenchymal stem cells inhibit differentiation and function of monocyte-derived dendritic cells. *Blood* **105**, 4120, 2005.
25. Mizuguchi, T., Hui, T., Palm, K., Sugiyama, N., Mitaka, T., Demetriou, A.A., and Rozga, J. Enhanced proliferation and differentiation of rat hepatocytes cultured with bone marrow stromal cells. *J Cell Physiol* **189**, 106, 2001.
26. Cao, Y., Ji, R.W., Davidson, D., Schaller, J., Marti, D., Sohndel, S., McCance, S.G., O'Reilly, M.S., Llinas, M., and Folkman, J. Kringle domains of human angiostatin. Characterization of the anti-proliferative activity on endothelial cells. *J Biol Chem* **271**, 29461, 1996.
27. Zhang, D., Kaufman, P.L., Gao, G., Saunders, R.A., and Ma, J.X. Intravitreal injection of plasminogen kringle 5, an endogenous angiogenic inhibitor, arrests retinal neovascularization in rats. *Diabetologia* **44**, 757, 2001.
28. Davidson, D.J., Haskell, C., Majest, S., Kherzai, A., Egan, D.A., Walter, K.A., Schneider, A., Gubbins, E.F., Solomon, L., Chen, Z., Lesniewski, R., and Henkin, J. Kringle 5 of human plasminogen induces apoptosis of endothelial and tumor cells through surface-expressed glucose-regulated protein 78. *Cancer Res* **65**, 4663, 2005.
29. O'Reilly, M.S., Holmgren, L., Shing, Y., Chen, C., Rosenthal, R.A., Moses, M., Lane, W.S., Cao, Y., Sage, E.H., and Folkman, J. Angiostatin: a novel angiogenesis inhibitor that mediates the suppression of metastases by a Lewis lung carcinoma. *Cell* **79**, 315, 1994.
30. Murphy, P.G., and Hart, D.A. Influence of exogenous growth factors on the expression of plasminogen activators and plasminogen activator inhibitors by cells isolated from normal and healing rabbit ligaments. *J Orthop Res* **12**, 564, 1994.
31. Mori, L., Bellini, A., Stacey, M.A., Schmidt, M., and Mattoli, S. Fibrocytes contribute to the myofibroblast population in wounded skin and originate from the bone marrow. *Exp Cell Res* **304**, 81, 2005.
32. Ishii, G., Sangai, T., Sugiyama, K., Ito, T., Hasebe, T., Endoh, Y., Magae, J., and Ochiai, A. *In vivo* characterization of bone marrow-derived fibroblasts recruited into fibrotic lesions. *Stem Cells* **23**, 699, 2005.
33. Yamaguchi, Y., Kubo, T., Murakami, T., Takahashi, M., Hakamata, Y., Kobayashi, E., Yoshida, S., Hosokawa, K., Yoshikawa, K., and Itami, S. Bone marrow cells differentiate into wound myofibroblasts and accelerate the healing of wounds with exposed bones when combined with an occlusive dressing. *Br J Dermatol* **152**, 616, 2005.
34. Fathke, C., Wilson, L., Hutter, J., Kapoor, V., Smith, A., Hocking, A., and Isik, F. Contribution of bone marrow-derived cells to skin: collagen deposition and wound repair. *Stem Cells* **22**, 812, 2004.
35. Hsu, C., and Chang, J. Clinical implications of growth factors in flexor tendon wound healing. *J Hand Surg [Am]* **29**, 551, 2004.
36. Wagner, M., Luhrs, H., Kloppel, G., Adler, G., and Schmid, R.M. Malignant transformation of duct-like cells originating from acini in transforming growth factor transgenic mice. *Gastroenterology* **115**, 1254, 1998.

Address reprint requests to:  
 Norimasa Iwasaki, M.D., Ph.D.  
 Department of Orthopaedic Surgery  
 Hokkaido University School of Medicine  
 Kita-15, Nishi-7, Kita-ku  
 Sapporo, Hokkaido, 060-8638  
 Japan

E-mail: niwasaki@med.hokudai.ac.jp

## The role of osteopontin in tendon tissue remodeling after denervation-induced mechanical stress deprivation

Noriaki Mori<sup>a</sup>, Tokifumi Majima<sup>a</sup>, Norimasa Iwasaki<sup>a</sup>, Shigeyuki Kon<sup>b</sup>, Kiyoshi Miyakawa<sup>c</sup>, Chiemi Kimura<sup>b</sup>, Kunio Tanaka<sup>c</sup>, David T. Denhardt<sup>d</sup>, Susan Rittling<sup>e</sup>, Akio Minami<sup>a</sup>, Toshimitsu Uede<sup>b,\*</sup>

<sup>a</sup> Department of Orthopaedic Surgery, Hokkaido University School of Medicine, Sapporo, Japan

<sup>b</sup> Division of Molecular Immunology, Institute for Genetic Medicine, Hokkaido University, Kita-15 Nishi-7 Kita-Ku, Sapporo, Hokkaido, 060-0815, Japan

<sup>c</sup> Central Laboratory for Research and Education, Asahikawa Medical College, Asahikawa, Japan

<sup>d</sup> Department of Cell Biology and Neuroscience, Rutgers University, Piscataway, New Jersey 08854, United States

<sup>e</sup> Department of Genetics, Rutgers University, Piscataway, New Jersey 08855, United States

Received 7 April 2006; received in revised form 28 August 2006; accepted 6 September 2006

### Abstract

It has been shown that musculoskeletal tissues undergo dynamic tissue remodeling by a process that is quite sensitive to the mechanical environment. However, the detailed molecular mechanism underlying this process remains unclear. We demonstrate here that after denervation-induced mechanical stress deprivation, tendons undergo dynamic tissue remodeling as evidenced by a significant reduction of the collagen fibril diameter. Importantly, the transient up-regulation of osteopontin (OPN) expression was characteristic during the early phase of tendon tissue remodeling. Following this dynamic change of OPN expression, matrix metalloproteinase (MMP)-13 expression was induced, which presumably accounts for the morphological changes of tendon by degrading tendon collagen fibrils. The modulation of MMP-13 expression by OPN was specific, since the expression of MMP-2, which is also known to be involved in tissue remodeling, did not alter in the tendons under the absence or presence of OPN. We also demonstrate that the modulation of MMP-13 expression by OPN is due to the signaling through cell surface receptors for OPN. Thus, we conclude that OPN plays a crucial role in conveying the effect of denervation-induced mechanical stress deprivation to the tendon fibroblasts to degrade the extracellular matrices by regulating MMP-13 expression in tendon fibroblasts.

© 2006 Elsevier B.V./International Society of Matrix Biology. All rights reserved.

**Keywords:** Osteopontin; Tendon remodeling; Mechanical stress deprivation; Matrix metalloproteinase-13

### 1. Introduction

Bone and muscle provide mechanical support for movement under gravitational and mechanical stress. The structure, organization, and remodeling of bone and muscle are sensitive to the mechanical environment as evidenced by the bone loss and muscle atrophy in bedridden patients as well as the increase in bone and muscle mass in athletes participating in high impact sports. Tendon tissues connect muscle to bone and allow transmission of forces generated by muscle to bone and provide motion and mechanical support to the joints. As in bone and muscle, mechanical loading improves the tensile strength, stiffness,

weight and cross-section area of tendons, and these effects can be explained by an increase in collagen and extracellular matrix synthesis by tendon cells (Kannus et al., 1992, 1997; Majima et al., 1996, 2003). However, the molecular mechanism coupling mechanical stress to tendon tissue remodeling remains unclear.

Osteopontin (OPN), also called early T lymphocyte activation-1 (Eta-1) or secreted phosphoprotein 1 (Spp1), was originally identified as a noncollagenous matrix protein in bone (Franzen and Heinegard, 1985; Singh et al., 1990). This cytokine and mineral matrix protein plays an important role in a number of physiological and pathological events, including tissue repair, regulation of bone metabolism, and inflammation and immunity (Denhardt et al., 2001b; Diao et al., 2004; Liaw et al., 1995; O'Regan and Berman, 2000; Sodek et al., 2000; Uede et al., 1997). Recent studies have shown that OPN is a crucial factor

\* Corresponding author. Tel./fax: +81 11 706 7542.

E-mail address: [toshi@igm.hokudai.ac.jp](mailto:toshi@igm.hokudai.ac.jp) (T. Uede).

triggering bone remodeling (Asou et al., 2001; Denhardt et al., 2001a; Ishijima et al., 2001; Meazzini et al., 1998; Rittling et al., 1998; Terai et al., 1999). In addition, disorganization of collagen and decreases in collagen type I content were observed in mice lacking OPN in the model of skin incision/wound healing (Liaw et al., 1998). Furthermore, OPN was highly up-regulated during the muscle regeneration process induced by injection of the snake venom, cardiotoxin (Hirata et al., 2003).

Musculoskeletal tissue cells, including osteoblasts, chondrocytes, myoblasts and skin and tendon fibroblasts, arise from differentiated mesenchymal stem cells (Salingcarnboriboon et al., 2003; Sharma and Maffulli, 2005). Thus, the musculoskeletal tissues are categorized as the same functional unit developed from the mesenchymal stem cells. This theoretical background and the data mentioned above led us to hypothesize that OPN could regulate tendon tissue remodeling in response to mechanical stress. To test this hypothesis, a denervation-induced mechanical stress deprivation model of the patellar tendon was used to evaluate the role of OPN during tendon tissue remodeling. The specific objectives of this study were 1) to detect OPN protein expression in normal tendon, 2) to examine the kinetics of OPN mRNA expression in the patellar tendon after mechanical stress deprivation, 3) to analyze the fine structure of patellar tendon after mechanical stress deprivation either in the presence or absence of OPN, and 4) to clarify a mechanism underlying OPN-induced tendon remodeling. The results shown in this paper provide the essential information on the role of OPN in musculoskeletal soft tissue remodeling responding to mechanical stress. Furthermore, this knowledge can be applied to the development of novel tactics for the treatment of various musculoskeletal soft tissue diseases involving abnormal tissue remodeling.

## 2. Results

### 2.1. Detection of OPN expression in tendon fibroblasts

In reverse transcriptase-polymerase chain reaction (RT-PCR) analysis, OPN mRNA expression was clearly detected in normal patellar tendon of wild-type (WT) mice, which had been kept under a physiological gravitational environment (Fig. 1A). Immunohistochemical analysis demonstrated that OPN protein expression was detected in tendon fibroblasts, which existed in the interstitial space of the tendons of WT mice (Fig. 1B–D). OPN protein expression was not detected in the patellar tendon of osteopontin-deficient ( $OPN^{-/-}$ ) mice (Fig. 1E). We further examined whether cultured tendon fibroblasts could secrete OPN *in vitro*. The cultured tendon fibroblasts from the normal patellar tendon secreted significant amounts of OPN protein ( $608.7 \pm 86.5$  ng/ml) into the culture medium. As expected, no OPN protein was found in culture supernatants of the tendon fibroblasts from mice lacking OPN.

### 2.2. Denervation-induced stress deprivation of patellar tendon

Physical tension of tendon is controlled by contraction of quadriceps femoris muscle, which is innervated by the fem-

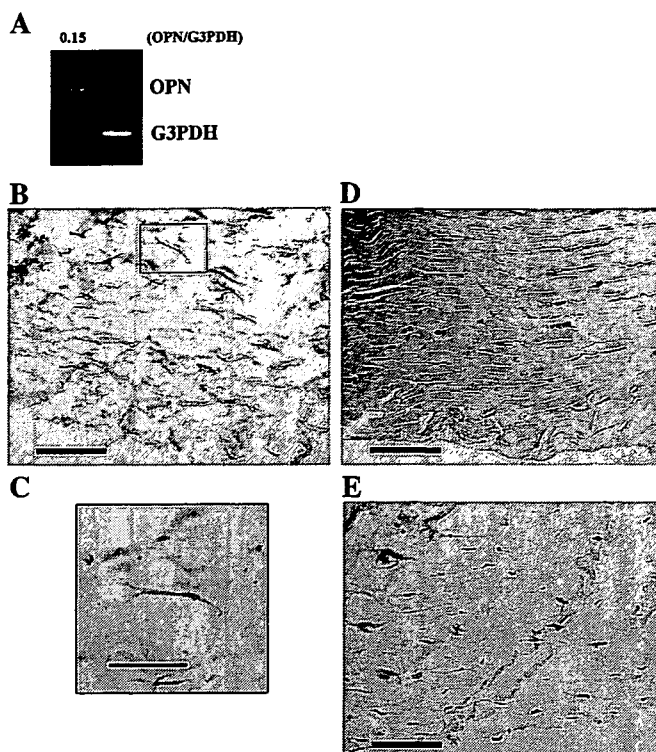


Fig. 1. Expression of OPN in normal patellar tendon in wild-type (WT) mice. (A) Total RNA was isolated from the homogenized samples of 21 patellar tendons from WT mice. RT-PCR shows the expression of OPN mRNA in normal loaded patellar tendon. The RT-PCR for G3PDH was used as a control. The number indicates the relative expression level of OPN mRNA against G3PDH. (B) Immunohistochemical staining of the sections obtained from the patellar tendon tissues of WT mice. (C) Magnified view of OPN-positive fibroblasts in the boxed region in B. (D) Hematoxylin–eosin (HE) staining of respective sections in B. (E) Immunohistochemical staining of the sections obtained from patellar tendon tissues of  $OPN^{-/-}$  mice. Scale bars indicate 50  $\mu$ m.

oral nerve. Thus, it is expected that the contraction of quadriceps femoris muscle can be abolished by transection of the femoral nerve, which leads to mechanical stress deprivation of patellar tendon. Surgery was performed under general anesthesia with pentobarbital sodium via intraperitoneal injection at 25 mg/kg body weight. A longitudinal skin incision was made over the proximal part of right medial thigh. To eliminate the effect of femoral nerve regeneration and inflammation on patellar tendon, a 1.0-cm segment of right femoral nerve was microscopically excised at the inguinal region (Fig. 2A, B). Before the excision of the femoral nerve, electromyography showed that the stimuli of the right femoral nerve elicited electric activity in right quadriceps femoris muscle. We confirmed that the stimuli of the femoral nerve did not elicit the electric activity in quadriceps femoris muscle after denervation. We also examined whether the transection of the femoral nerve induces inflammatory reactions in tendon. Histologically, there was no inflammatory cell infiltration in tendon at day 7 (Fig. 2D). This was confirmed by absence of F4/80-positive macrophages in tendon tissues at days 1, 3, 7 and 14 after mechanical stress deprivation (Fig. 2D, E). At day 42 after stress deprivation, we

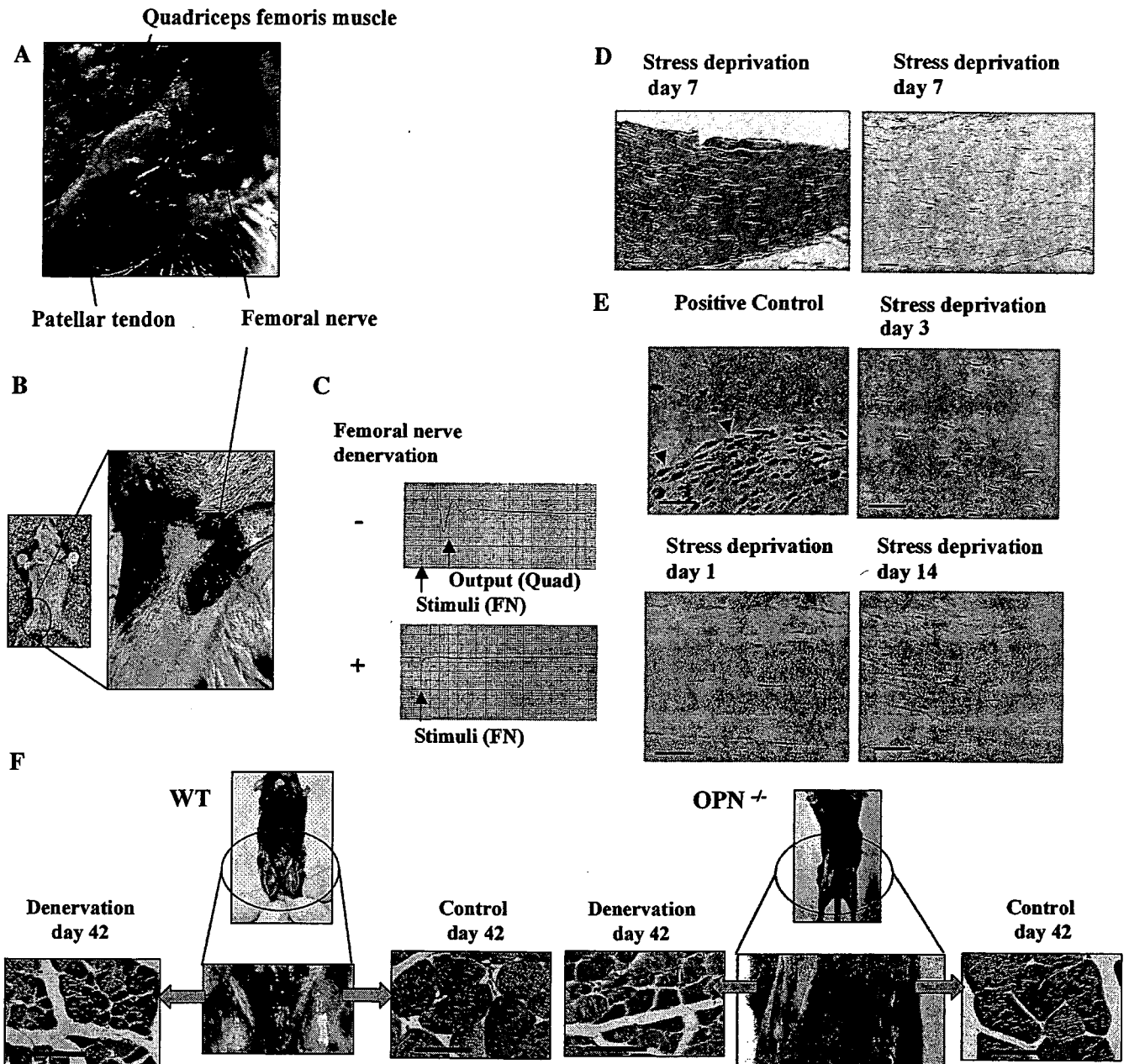


Fig. 2. Denervation-induced stress deprivation model of the patellar tendon. (A) Macroscopic anatomy of the proximal part of mouse lower extremity. (B) Right panel, an enlarged view of the region in the circled portion in left panel, shows femoral nerve exposed by small incision over the proximal part of the right medial thigh. The femoral nerve was microscopically transected at the inguinal region. (C) Electromyographic investigation to confirm the patellar tendon of denervation-induced stress deprivation. When femoral nerve is stimulated before denervation (upper panel), electrical activity is recorded in the quadriceps femoris muscle, while that is not detected after denervation (lower panel). FN, femoral nerve; Quad, quadriceps femoris muscle. (D) No inflammatory cell infiltration in stress deprived tendon after denervation. HE staining (left) and F4/80 staining (right) of tendon sections at day 7 after stress deprivation. (E) F4/80 staining of tendon sections at days 1, 3 and 14 after stress deprivation. Inflammatory synovial tissue of mice was used as a positive control and arrowheads indicate F4/80-positive cells. Scale bars indicate 50  $\mu$ m. Data are representative of several independent experiments. (F) Light micrographs of the transverse sectioned quadriceps femoris muscle obtained from WT (left panels) and  $OPN^{-/-}$  mice (right panels) at day 42 after stress deprivation. Sections were stained with hematoxylin–eosin (HE). Scale bars indicate 50  $\mu$ m. Macroscopic views of right and control left quadriceps muscles in both WT and  $OPN^{-/-}$  mice were also shown.

showed that atrophy of right quadriceps femoris muscle was induced (Fig. 2F) as described previously (Zhang et al., 2006). Thus, patellar tendon load is selectively deprived by denervation-induced muscle atrophy. Using this model, we evaluated the role of OPN during the course of tendon tissue remodeling after stress deprivation.

### 2.3. Lack of OPN prevents stress deprivation-induced decrease in collagen fibril diameter of patellar tendon

The morphological analysis of tendons by transmission electron microscopy (TEM) demonstrated that the diameter of the collagen fibrils significantly decreased in WT mice at

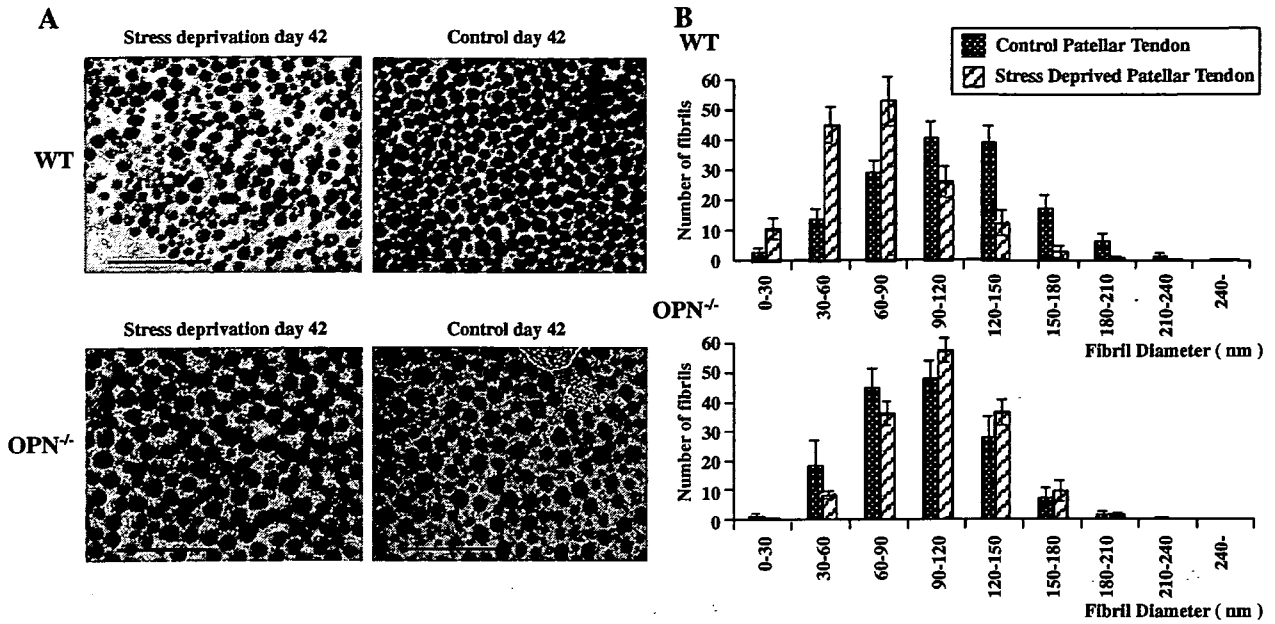


Fig. 3. Transmission electron micrographs (TEM) of collagen fibril morphology in normal loaded and stress deprived patellar tendon. (A) Upper panel shows the micrographs of stress deprived patellar tendon (left) and contralateral normal patellar tendon (right) in WT mice at day 42 after stress deprivation. Lower panel shows micrographs of stress deprived patellar tendon (left) and contralateral normal patellar tendon (right) in OPN<sup>-/-</sup> mice at day 42. Scale bars indicate 1  $\mu$ m. (B) Histogram profiles of the collagen fibril diameter in WT mice ( $n=8$ ) and OPN<sup>-/-</sup> mice ( $n=10$ ) at day 42.

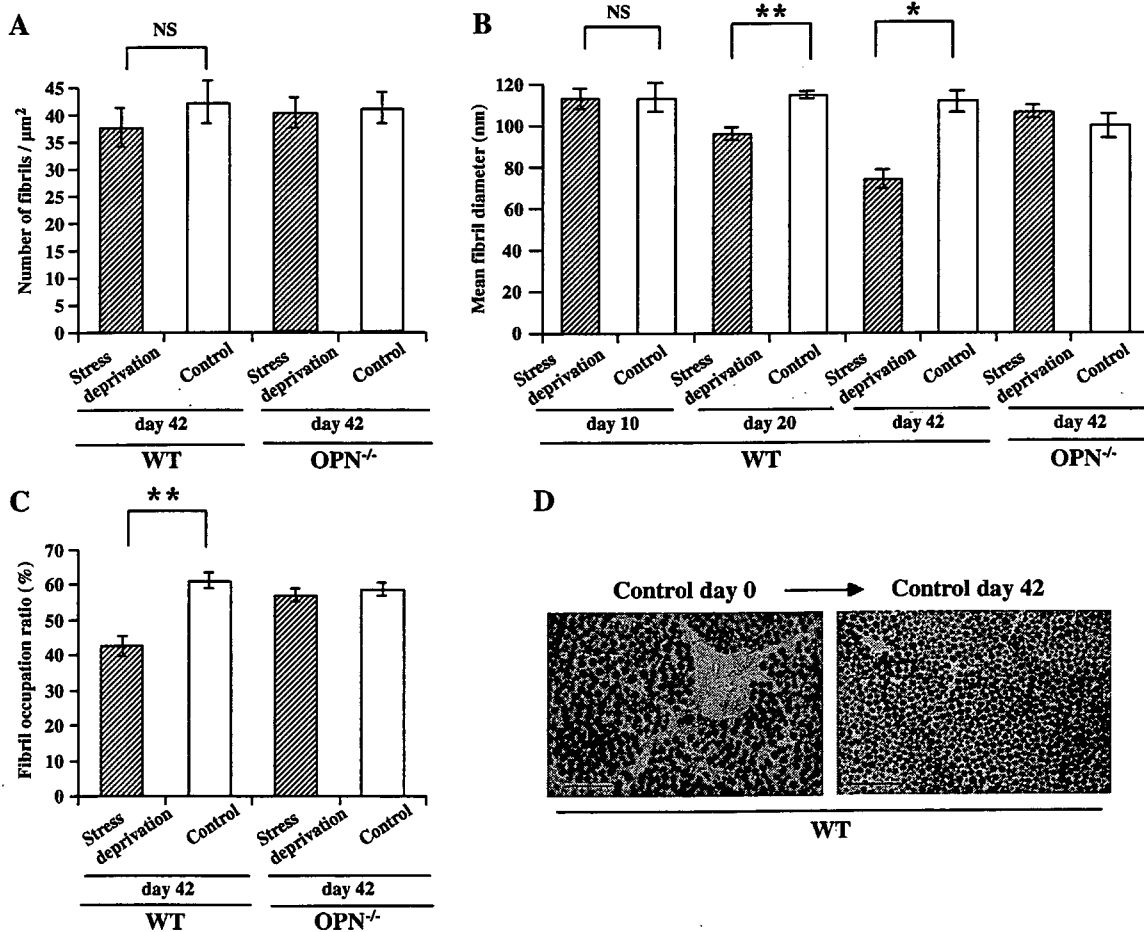


Fig. 4. Quantitative analyses from ultrastructural observations of patellar tendons in WT mice ( $n=5, 5, \text{ and } 8$  at days 10, 20 and 42, respectively) and OPN<sup>-/-</sup> mice ( $n=10$ ) at days 10, 20, or 42 after stress deprivation. (A) Number of fibrils/ $\mu$ m<sup>2</sup> at day 42. (B) Mean collagen fibril diameter (nm) at days 10, 20, or 42. (C) Fibril occupation ratio (%) at day 42. (D) Left panel is preoperative normal loaded patellar tendon and right panel is control patellar tendon at day 42 after surgery in WT mice. Scale bars indicate 1  $\mu$ m. \* $P<0.05$  versus control; \*\* $P<0.001$  versus control; NS, not significantly different.



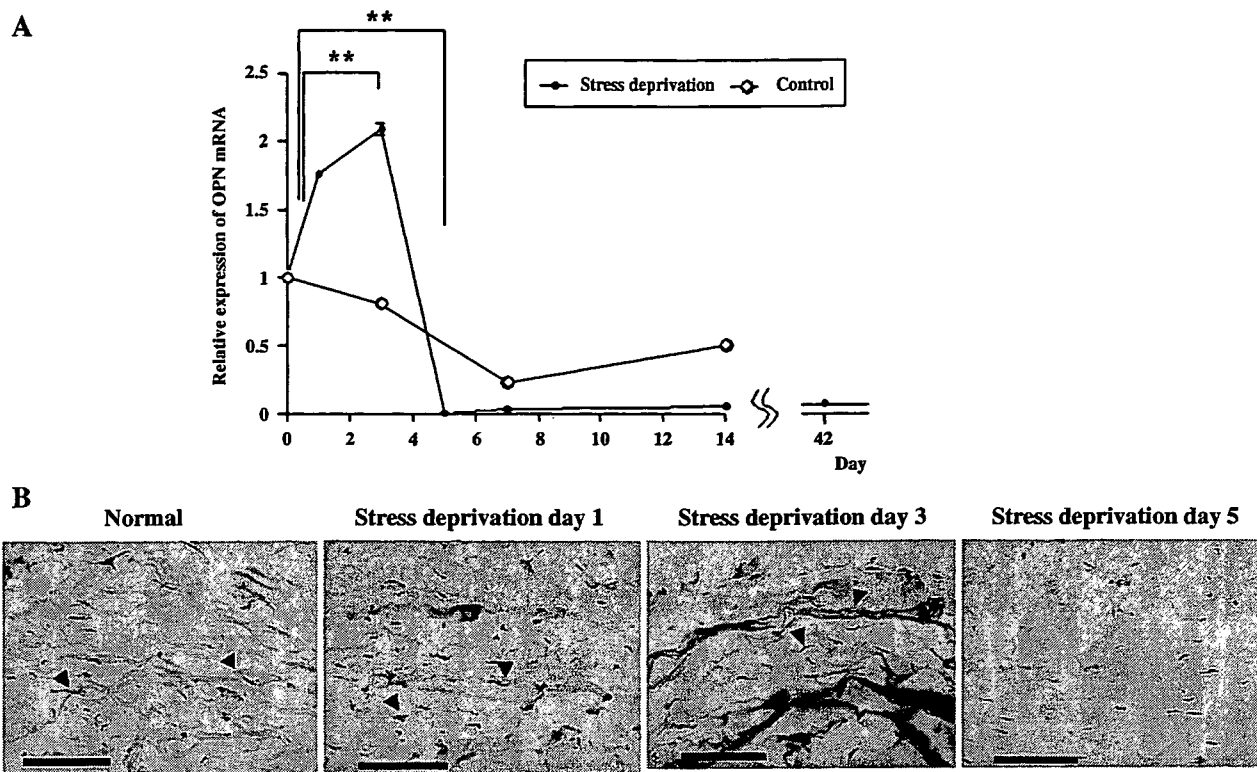


Fig. 5. Changes in the expression level of OPN in tendon of WT mice after stress deprivation. (A) Real-time PCR was conducted at indicated times after stress deprivation of the tendon. Expression of OPN mRNA was normalized by G3PDH. Total RNA was isolated from the homogenized samples of ten stress deprived patellar tendons at days 0, 1, 3, 5, 7, and 42 after surgery and ten control patellar tendons at days 0, 3, 7, and 14 after surgery.  $n=3$ ,  $**P<0.001$  versus day 0. (B) Immunohistology of OPN expression by patellar tendon fibroblasts at days 0, 1, 3, and 5 after stress deprivation. Arrowheads indicate positive staining. Scale bars indicate 50  $\mu\text{m}$ .

42 days after the denervation-induced stress deprivation of the tendon, as compared to those of the control contralateral tendon of the same mouse (Fig. 3A). In contrast, in mice lacking OPN, the stress deprivation-induced decrease in diameter of tendon collagen fibril was not detected. At day 42, the diameter of the tendon collagen fibrils was very similar between the stress deprived right tendon and the left tendon that was still responsive to mechanical stress (Fig. 3A).

To quantify the morphological change of tendon collagen fibrils after stress deprivation, a detailed analysis was performed. Although the distribution of collagen fibril diameters at 42 days after stress deprivation was shifted to smaller diameters in WT mice, no such alteration was found in mice lacking OPN (Fig. 3B). The apparent left shift in the collagen fibril size suggests the loss of large fibers and a gain of small fibers with stress deprivation in WT mice.

In this regard, it should be noted that the number of fibrils was not significantly different between stress deprived and control loaded tendons in WT mice (Fig. 4A), indicating that the appearance of small diameter collagen fibrils newly synthesized may not account for the apparent left shift in the collagen fiber size. In addition, mean collagen fibril diameter and fibril occupation ratio per given area were significantly decreased in stress deprived tendons at day 42, as compared to

those of control loaded tendons ( $111.6\pm 5.2$  nm versus  $74.4\pm 4.6$  nm (Fig. 4B) and  $61.2\pm 2.3\%$  versus  $42.6\pm 2.7\%$  (Fig. 4C), respectively). These results indicated that pre-existed collagen fibers were forced to reduce diameter of collagen fibrils in WT mice. It is also possible that control contralateral tendon is subjected to mechanical overloading, which leads to the increase of collagen fibril diameter. This overloading may explain the difference in collagen fibril diameter between stress deprived and control loaded tendons. Therefore, we examined whether the diameter of collagen fibrils in control tendons differ between before and after stress deprivation. We found that collagen fibril diameter did not differ significantly between day 0 and day 42 tendons (Fig. 4D). Nevertheless, in mice lacking OPN, there were no significant differences in collagen fibril diameter and fibril occupation ratio between stress deprived tendon and control tendon at 42 days (Fig. 4B, C). In order to further clarify the time point when fibril diameter change occurs, we additionally obtained tendons of WT mice at 10 and 20 days post-operation. We found that there were significant differences in collagen diameter at 20 days, but not 10 days after operation (Fig. 4B). These data demonstrate that OPN is involved in the process of tendon remodeling after stress deprivation. In order to clarify the mechanism how OPN regulates the process of tendon remodeling, we examined the kinetics of OPN mRNA expression in tendon after unloading.

#### 2.4. The kinetics of OPN gene expression in tendon after denervation-induced stress deprivation

At days 0, 1, 3, 5, 7, 14, and 42 after stress deprivation, the expression of OPN mRNA in patellar tendon was examined. By quantitative real-time PCR analysis, we found that normal tendon expressed OPN mRNA. Importantly, OPN expression was up-regulated at day 1 and day 3 ( $n=3$ ,  $P<0.001$ ) after stress deprivation and then declined significantly at day 5 ( $n=3$ ,  $P<0.001$ ). The level of OPN expression at day 5 was not up-regulated, but rather lower than that of normal tendon ( $n=3$ ,  $P<0.001$ ), and it remained suppressed even up to day 42 after stress deprivation. In control contralateral tendon, such dynamic changes in OPN expression were not detected (Fig. 5A). Consistent with these data, we demonstrated that OPN protein expression was detected in normal tendon and tendon tissues at days 1 and 3 after stress deprivation. However, at day 5 OPN protein expression was not detected (Fig. 5B).

#### 2.5. Lack of significant contribution of collagen synthesis and apoptosis for the decrease of collagen fibril diameter of tendon after mechanical stress deprivation

OPN might modulate the process of tendon remodeling in various ways. It has been shown that OPN regulates collagen synthesis and accumulation during myocardial remodeling (Trueblood et al., 2001). We therefore tested whether a decrease in collagen synthesis could explain the decrease in collagen fibril diameter in tendon of WT mice after stress deprivation. The real-time PCR analysis demonstrated that collagen mRNA synthesis decreased at days 3 and 14 in both stress deprived tendon and control contralateral loaded tendons, as compared to that in tendon at day 0 (without surgery). However, importantly, the values do not differ significantly between stress deprived tendon and contralateral loaded tendon (Fig. 6A), indicating that the decrease of collagen mRNA synthesis may not account for the decrease in collagen fibril diameter of tendon after stress deprivation.

OPN is also involved in the regulation of cell apoptosis (Khan et al., 2002; Weintraub et al., 2000; Zohar et al., 2004). As shown in Fig. 5A, a dynamic change of OPN expression was observed during the early phase of tissue remodeling in stress deprived tendon. Therefore, we examined for the presence of TUNEL-positive cells at days 0, 3, and 7 after stress deprivation. As shown in Fig. 6B, apoptotic cells were not detected in WT mice. Results suggested that an increase in apoptosis of tendon fibroblasts does not significantly contribute to the decrease in collagen fibril diameter in stress deprived tendon.

#### 2.6. The dynamic regulation of MMP-13 expression during the course of tendon remodeling after stress deprivation

MMPs play a critical role during the course of tissue remodeling. Among the major factors in the remodeling process, collagenases are considered to predominantly degrade the native interstitial collagens in tendon tissue (Chung et al.,

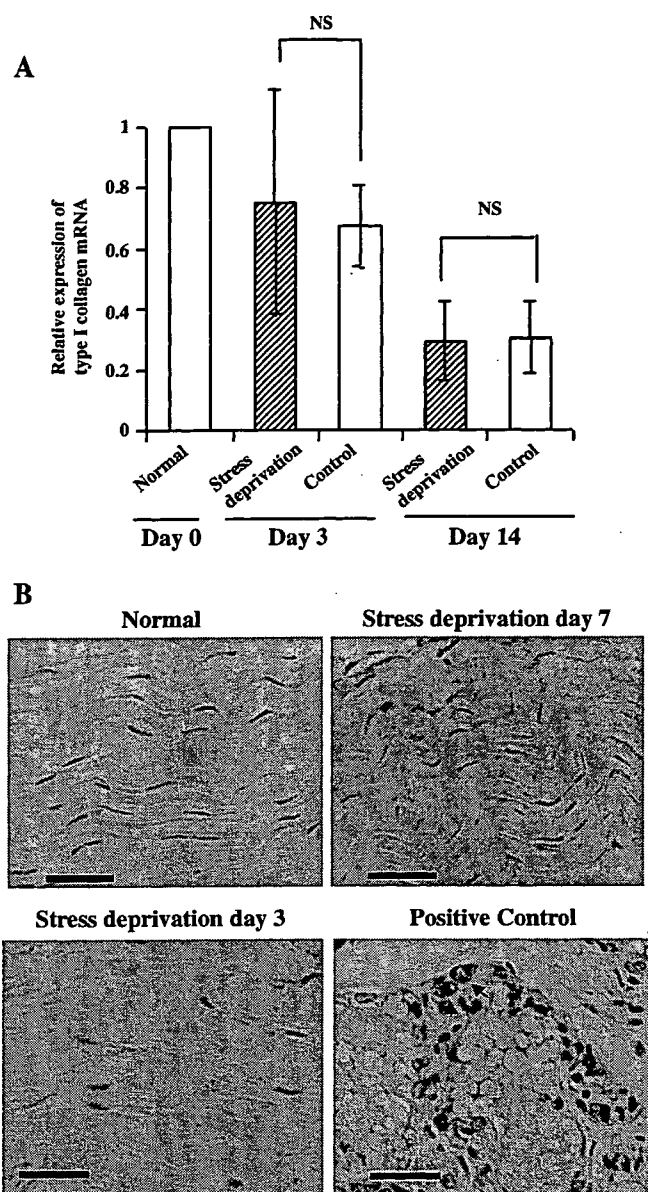


Fig. 6. Lack of significant contribution of collagen mRNA synthesis and apoptosis for the decrease of collagen fibril diameter after stress deprivation. (A) Real-time PCR analysis of type I collagen mRNA expression in WT mice was conducted at days 0, 3, and 14 after mechanical stress deprivation ( $n=4$ , NS, not significantly different). Expression of OPN mRNA was normalized by G3PDH. (B) Terminal deoxynucleotidyltransferase-mediated dUTP end labeling (TUNEL) assay was conducted at days 0, 3 and 7 after stress deprivation. Mammary ground tissue in mice was used as a positive control. Arrowheads indicate TUNEL-positive cells. Scale bars indicate 50  $\mu\text{m}$ .

2004; Cunningham et al., 1999; Jain et al., 2002). In addition, it has been shown that OPN negatively and positively regulates MMPs expression (D'Alonzo et al., 2002; Philip et al., 2001; Rangaswami et al., 2004). Therefore, we analyzed the expression level of the genes encoding collagenase-3 (MMP-13) and as a control, MMP-2 in WT mice. MMP-13 mRNA expression was very low up to day 3 after stress deprivation, and then dramatically increased up to day 14 (20-fold increase at day 14). At day 21, the degree of MMP-13 expression returned to the basal level (Fig. 7A). It should be noted that augmentation

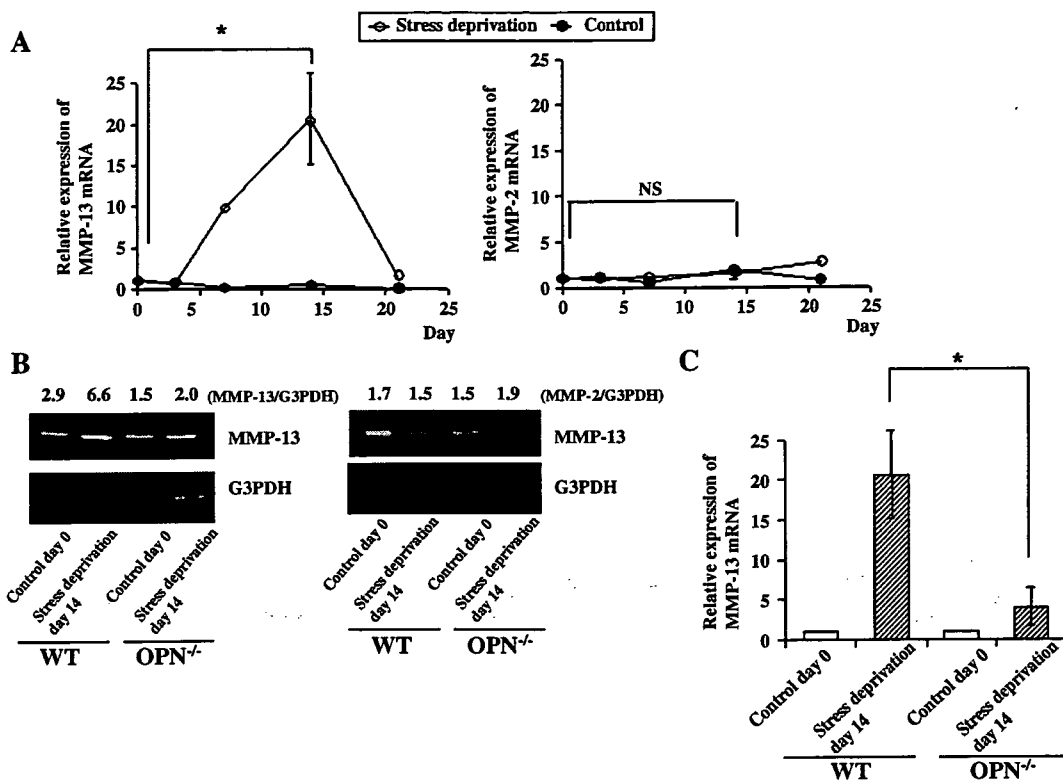


Fig. 7. Change of the expression level of MMP-13 and -2 genes in stress deprived tendons of WT mice and OPN<sup>-/-</sup> mice. (A) Real-time PCR analyses of MMP-13 (left panel) and -2 (right panel) mRNA expression in stress deprived and control loaded tendons of WT mice at indicated time points ( $n=4$ ,  $*P<0.05$  versus day 0. NS, not significantly different). (B) RT-PCR analysis of MMP-13 (left panel) and -2 (right panel) expression at day 0 and day 14 after stress deprivation in both WT and OPN<sup>-/-</sup> mice. The numbers indicate the relative expression level of OPN mRNA against G3PDH. (C) Quantitative real-time PCR analysis of MMP-13 mRNA expression in tendon at day 0 and day 14 after stress deprivation ( $n=4$ ,  $*P<0.05$ ) in both WT and OPN<sup>-/-</sup> mice.

of MMP-13 expression was not seen in control contralateral loaded tendons. This dynamic change in gene expression was not found for MMP-2 (Fig. 7A). It should be noted that prior to the augmentation of MMP-13 expression, OPN expression was transiently up-regulated at day 3 and sharply declined thereafter (Fig. 5A). Therefore, we investigated whether OPN was involved in MMP-13 gene expression during tendon remodeling after stress deprivation, by comparing the expression level of MMP-13 in tendons of WT and OPN<sup>-/-</sup> mice. First, we performed RT-PCR analysis to detect MMP-2 and MMP-13 expression in stress deprived tendons of WT mice and OPN<sup>-/-</sup> mice. MMP-2 expression at stress deprivation day 14 was not significantly augmented in both WT and OPN<sup>-/-</sup> mice, compared to those at control day 0. In contrast, MMP-13 expression was augmented at day 14 as expected in WT mice, while this augmentation was not detected in OPN<sup>-/-</sup> mice (Fig. 7B). To quantitate the level of MMP-13 expression, we carried out real-time PCR analysis. We found that MMP-13 gene expression was increased 20.7-fold at day 14 after stress deprivation in WT mice but only 4.1-fold in OPN<sup>-/-</sup> mice (Fig. 7C).

The interpretation of data shown in Figs. 5A and 7A is ambivalent. Naturally, the high concentration of OPN may up-regulate MMP-13 expression. However, one can argue that the sharp decline of OPN concentration is required for the up-regulation of MMP-13 expression. In this scenario, exogenous

OPN may down-regulate MMP-13 expression. In order to analyze how OPN regulate MMP expression, we set up an *in vitro* system using cultured tendon fibroblasts. Cultured tendon fibroblasts secreted OPN as described above and expressed a low level of MMP-13 (Fig. 8A). We assumed that secreted OPN bound to its cell surface receptor on fibroblasts. Importantly, MMP-13 expression was significantly augmented by the addition of synthetic peptides, GRGDS, which interfere with the binding of OPN to its receptor, but not GRGES (Fig. 8A). Furthermore, an anti- $\alpha v$  integrin antibody that interferes with the binding of OPN to its receptor  $\alpha v \beta 3$  could also augment MMP-13 expression (Fig. 8A). We also inhibit the interaction of OPN and its integrin receptor by anti-OPN antibody (M5). M5, but not control M3 antibody augmented MMP-13 expression (Fig. 8A). To maximize the OPN-mediated signaling, we added exogenous OPN to the culture and found that the MMP-13 expression by tendon fibroblasts was down-regulated by exogenous OPN (Fig. 8A). Cultured tendon fibroblasts of OPN-deficient mice also expressed very low level of MMP-13 (Fig. 8B). Since endogenous OPN-mediated signaling is missing in those cells, we added exogenous OPN to the culture and found that MMP-13 expression was further down-regulated (Fig. 8B). Importantly, the interference of interaction with exogenous OPN and its receptor on fibroblasts of OPN-deficient mice by M5 antibody resulted in a significant up-regulation of MMP-13 expression, but not by control M3

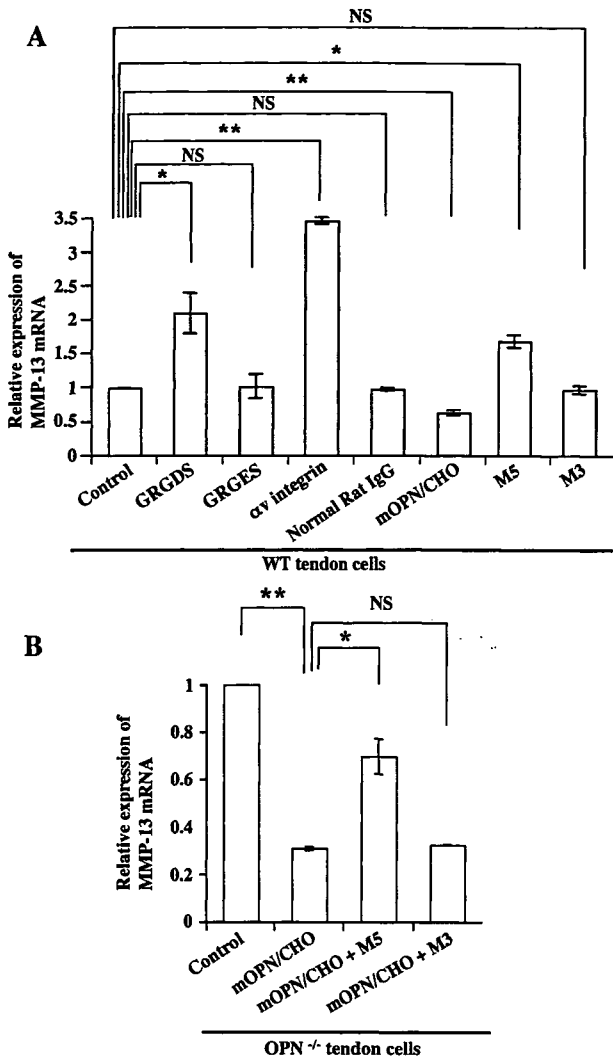


Fig. 8. Up-regulation of MMP-13 expression by abrogation of interaction between OPN and its receptors. (A) The tendon fibroblasts of WT mice ( $2 \times 10^4$  cells/ml) were cultured under serum-starved conditions with 100  $\mu$ g/ml GRGDS, 100  $\mu$ g/ml GRGES peptide, 50  $\mu$ g/ml anti- $\alpha$ v integrin antibody, 50  $\mu$ g/ml control rat IgG, 30  $\mu$ g/ml M5 antibody, 30  $\mu$ g/ml M3 antibody, or 10  $\mu$ g/ml purified mouse OPN (mOPN/CHO) for 48 h. Total RNA was extracted and MMP-13 mRNA expression was measured by real-time PCR ( $n=3$ ,  $*P<0.05$  versus control;  $**P<0.001$  versus control; NS, not significantly different). (B) The tendon fibroblasts of OPN<sup>-/-</sup> mice ( $2 \times 10^4$  cells/ml) were cultured under serum-starved conditions in the absence or presence of 10  $\mu$ g/ml purified mouse OPN (mOPN/CHO) for 48 h. In some experiments, 30  $\mu$ g/ml M5 or 30  $\mu$ g/ml M3 antibody was included in the culture. Total RNA was extracted and MMP-13 mRNA expression was measured by real-time PCR ( $n=3$ ,  $**P<0.001$  versus control).

antibody (Fig. 8B). Taken together, OPN negatively regulated MMP-13 expression through its integrin receptor.

### 3. Discussion

This study demonstrated that, after denervation-induced stress deprivation, tendons underwent dynamic tissue remodeling as evidenced by the significant reduction of the constituent collagen fibril diameter. However, in the absence of OPN, such morphological alterations were not evident. Our results indicate that OPN plays a crucial role in regulating tendon remodeling

induced by stress deprivation. It should be noted that augmentation of OPN mRNA expression lasted only for 3 days, indicating that OPN is involved in the initial early molecular events during the course of tendon remodeling. Since tendon is categorized as the same functional compartment, including bones and muscles, and shares the common stem cells with these tissues, our findings are consistent with the previous reports, where OPN gene expression was detected in early phases of bone remodeling and muscle regeneration (Denhardt et al., 2001a; Hirata et al., 2003; Nomura and Takano-Yamamoto, 2000; Terai et al., 1999). The tissue remodeling involves both degradation of extracellular matrix proteins and synthesis of new matrix components. In addition, denervation-induced stress deprivation results in the reduction of mechanical strength of stress deprived patellar tendon and the reduction of elastic modulus is associated with the up-regulation of interstitial collagenases (MMP-1, -8 and -13) in tendon (Arnoczky et al., 2004; Lavagnino et al., 2005; Majima et al., 2000). Importantly, these collagenases (MMP-1, -8 and -13) are capable of unwinding and degrading type I collagen, the major component (>90%) of tendon tissue (Chung et al., 2004; Cunningham et al., 1999; Jain et al., 2002). MMP-8 is mainly produced by neutrophils under inflammatory condition (Balbin et al., 1998; Hasty et al., 1990). We showed that our model did not involve neutrophil infiltration into tendons. It has been shown that rodents lack MMP-1 (collagenase-1) gene (Balbin et al., 2001; Henriot et al., 1992; Vincenti et al., 1998). Recently OPN has been linked to activation of MMP-2, MMP-3 and MMP-9 (Agnihotri et al., 2001; Fisher et al., 2004; Ogbureke and Fisher, 2004; Philip et al., 2001; Rangaswami et al., 2004), of which only MMP-2 and MMP-9 degrade type IV collagen, but not type I collagen. Therefore, we focused on MMP-13 and tested whether OPN could regulate MMP-13 (collagenase-3) in stress deprived tendon. We found that the mice lacking OPN did not augment MMP-13 expression during the course of tendon remodeling. However, importantly, we demonstrated that stress deprivation induced a transient, but significant up-regulation of OPN expression that preceded the subsequent up-regulation of MMP-13 gene expression in tendon of WT mice. It should be pointed out that collagen diameter thinning in tendon did not occur prior to the elevation of MMP-13 expression. Thus, it is reasonable to speculate that high OPN expression stimulates or is required for the subsequent up-regulation of MMP-13 expression and tendon remodeling. It is important to note that decreased collagen fibril diameter could be at least partially explained by altered collagen assembly in the presence of higher OPN levels in areas of new matrix synthesis in the tendons as reported previously (Liaw et al., 1998). The defected collagen assembly may lead to secretion of excess non-fibrillar (soluble) collagen into the matrix, which interacts with cell surface receptors and causes the up-regulation of MMP-13 as it has been shown in chondrocytes (Ronziere et al., 2005).

However, our results argued against the above hypothesis. We demonstrated that cultured tendon fibroblasts of WT mice secreted OPN and expressed low levels of MMP-13. It is possible that secreted OPN binds to its receptor expressed by